Am J Cancer Res 2021;11(6):2637-2653
www.ajcr.us /ISSN:2156-6976/ajcr0122610

Original Article

A naturally derived small molecule PSM0537 targets the AF1Q-TCF4 interaction to suppress COX2 expression and inhibit cell proliferation and metastasis in osteosarcoma

Ning Duan[1,2*], Wentao Zhang[2*], Tao Song[2], Zhong Li[2], Xun Chen[2], Wei Ma[1]

[1]Department of Orthopaedics, The First Affiliated Hospital of Xi'an Jiaotong University, Xi'an 710061, Shaanxi, China; [2]Department of Orthopaedic Surgery, Honghui Hospital, Xi'an Jiaotong University, Xi'an 710054, Shaanxi, China. [*]Equal contributors.

Received September 17, 2020; Accepted May 4, 2021; Epub June 15, 2021; Published June 30, 2021

Abstract: ALL1 fused gene from chromosome 1q (AF1Q) functions as an oncogene in several types of cancers, but it has not been observed in osteosarcoma. In this study, we revealed that AF1Q was overexpressed in multiple osteosarcoma cell lines, and its expression level increased with the severity of tumor malignancy in osteosarcoma biopsies. AF1Q was coupled with the transcription factor T cell factor 4 (TCF4) to assemble a complex to bind to the promoter of cyclooxygenase 2 (*COX2*) and activate its expression. The individual knockdown of *AF1Q*, *TCF4*, or *COX2* in osteosarcoma cell lines significantly decreased cell proliferation and invasion *in vitro*. The tumor xenograft model also indicated that the individual knockdown of *AF1Q*, *TCF4*, or *COX2* could inhibit tumor growth and metastasis. On the basis of these promising results, we established an *in vitro* AlphaScreen method to identify the compounds that disrupted the AF1Q-TCF4 interaction in a naturally derived small molecule pool. We discovered a compound called PSM0537, which showed a strong ability to inhibit the AF1Q-TCF4 interaction at a low dose of half-maximal inhibitory concentration (IC_{50}) (210.3 ± 15.6 nM). The administration of PSM0537 *in vitro* and *in vivo* could dramatically inhibit cell proliferation, invasion, and metastasis. Collectively, our findings reveal that the AF1Q-TCF4 transcriptional complex controls the expression of *COX2* and that targeting the AF1Q-TCF4 interaction with PSM0537 could inhibit tumor cell growth and metastasis. Our results provide a new path for chemotherapy of osteosarcoma.

Keywords: AF1Q, TCF4, COX2, PSM0537, osteosarcoma, cell proliferation, metastasis

Introduction

Osteosarcoma is the most common tumor occurring in bones and is prevalent among children and adolescents [1]. According to the tumor, nodes, and metastases (TNM) staging system, osteosarcoma can be classified into I, IIA, IIB, and III [1-3]. Localized tumors belong to stages I and II, and metastatic tumors are under stage III [1-3]. Osteosarcoma is therapied with a combination of strategies that consist of surgery, chemotherapy, and radiation therapy [4]. For distant metastatic osteosarcoma, the five-year survival rate is only 27%, which is much lower than that of patients with localized and regional metastatic osteosarcoma tumors [4]. Therefore, discovering molecules that affect osteosarcoma metastasis and targeting these molecules with compounds may provide new strategies for the treatment of osteosarcoma.

ALL1 fused gene from chromosome 1q (AF1Q), also known as MLLT11 transcription factor 7 cofactor, is overexpressed in several cancers, including acute myeloid leukemia [5], colorectal cancer (CRC) [6], breast cancer [7], thyroid cancer [8], and testicular cancer [9]. Mechanically, AF1Q functions as an activator to induce the transduction of several signaling pathways, such as Wnt/β-catenin [10], protein kinase B/phosphatidylinositol (AKT/PI3K) [6], and platelet-derived growth factor receptor/signal transducer and activator of transcription 3 (PDGFR/

STAT3) [11]. During the metastasis of breast cancer, AF1Q has been reported to directly interact with T cell factor 7 (TCF7), thus activating the Wnt/β-catenin signaling and causing the transcriptional activation of CD44 (cluster of differentiation) [12]. AF1Q upregulates PDGFR signaling, which further enhances STAT3 activity through SRC (sarcoma) kinase activation [11]. Although AF1Q is known as a cofactor of the transcription factor, it is still largely unknown in terms of the AF1Q-associated transcription factors in different biological processes.

Cyclooxygenase 2 (COX2), also known as prostaglandin-endoperoxide synthase 2, has been shown to play a role in the different stages of tumorigenesis, such as tumor cell proliferation, angiogenesis, and metastasis [13]. COX2 accumulates in multiple cancers, including CRC [14, 15], breast cancer [16], hepatocellular carcinoma [17], pancreatic cancer [18], and osteosarcoma [19]. Elevated COX2 promotes cell proliferation by upregulating the epidermal growth factor receptor [20], inhibits apoptosis by controlling the expression of B-cell CLL/Lymphoma 2 (*BCL2*) [21], induce angiogenesis by increasing the expression levels of vascular endothelial growth factor and fibroblast growth factor [22], and facilitate metastasis by inducing matrix metallopeptidase 2 [23]. In osteosarcoma, the overexpression of *COX2* can increase tumor cell mobility, invasiveness, and distant metastasis, which significantly affects the post-metastatic survival of osteosarcoma patients [24]. Although *COX2* overexpression is prevalent in different cancers, the transcriptional regulatory mechanism of its overexpression is still unclear.

To investigate whether AF1Q was overexpressed in osteosarcoma, we examined its expression level in six osteosarcoma cell lines and 28 pairs of cancerous biopsies and non-cancerous tissues. We found that both mRNA and the protein levels of AF1Q were significantly overexpressed. Conducting a microarray analysis using two osteosarcoma cell lines (MG63 and U2OS) and their corresponding AF1Q-knockdown cells, we discovered that the down-regulation of *AF1Q* could decrease the *COX2* mRNA level. We then performed an immunoprecipitation (IP) assay to determine whether AF1Q could pull down the transcription factor TCF4. Using a co-immunoprecipitation (Co-IP) assay, luciferase assay, and chromatin immunoprecipitation (ChIP) assay, we revealed that AF1Q could interact with TCF4 to assemble a transcriptional complex, which bound to the promoter of *COX2* to activate the expression of *COX2*. We then evaluated the *in vitro* and *in vivo* effects of knocking down *AF1Q*, *TCF4*, and *COX2* on inhibiting tumor cell growth. In addition, we developed an *in vitro* AlphaScreen method to identify the small molecules that disrupted the interaction between AF1Q and TCF4. A compound called PSM0537 was identified, and the *in vitro* and *in vivo* effects on inhibiting tumor cell growth and metastasis were examined.

Materials and methods

Cell lines and cell culture

One osteoblast cell line hFOB1.19 (#CRL-11372) and six human osteosarcoma cell lines, including MG63 (#CRL-1427), KHOS (#CRL-1544), 143B (#CRL-8303), HOS (#CRL-1543), Saos2 (#HTB-85), and U2OS (#HTB-96), were purchased from the American Type Culture Collection (Manassas, VA, USA). All cells were cultured in Dulbecco's Modified Eagle Medium (DMEM) (Thermo Fisher, Shanghai, China, #10566016) supplemented with 10% fetal bovine serum (FBS) (Thermo Fisher, #1600044) and 100 $U \cdot mL^{-1}$ penicillin-streptomycin (Thermo Fisher, #15140148). The hFOB1.19 cells were incubated at 33°C, and the other cell lines were cultured at 37°C.

Cell transfection

To knock down genes, the MISSION shRNA lentiviral transduction particles of different genes, including *AF1Q* (Sigma-Aldrich, Shanghai, China, #TRCN0000318810), *TCF4* (#TRCN0000274214), and *COX2* (#TRCN0000294374), were respectively transfected into MG63 and U2OS cells with the FuGene 6 reagent (Promega, Shanghai, China, #E2691). A lentiviral transduction particle containing the pLKO.1 empty vector was used as the control. The transfected cells were recovered in an antibiotic-free DMEM medium for 6 h, followed by selection using DMEM + 1 μg/mL puromycin medium. The individual puromycin-resistant cells were collected and subjected to examining the knockdown efficiency of the target

genes. For plasmid transfection, 2 μg plasmid DNA was transfected into cells using the Lipofectamine 3000 reagent (Thermo Fisher, #L3000001), following the guidelines of the manufacturer.

Tissue collection

A total of 28 pairs of cancerous biopsies and their adjacent noncancerous tissues were collected from osteosarcoma patients under different TNM stages (n = 7 for each stage). Five healthy control tissues were collected from patients whose femurs were fractured and underwent surgery in the Department of Orthopedic Surgery, Xi'an Honghui Hospital. The basic characteristics of the osteosarcoma patients and controls are summarized in Table S1. All participants signed a consent form reviewed and approved by the ethical board of Xi'an Honghui Hospital, Shaanxi, China.

Microarray analysis

The hFOB1.19, MG63, U2OS, and the AF1Q-knockdown (KD) cells in both MG63 and U2OS backgrounds were subjected to isolate RNA using the NucleoSpin RNA Plus Kit (Takara, Beijing, China, #740984) according to the manufacturer's protocol. The purified RNA was used for quantification, and 1 μg RNA was subjected to a microarray analysis using the SurePrint G3 Human Gene Expression 8x60K v2 Microarray Kit (Agilent, Beijing, China, #G4851B). The procedures were the same as described previously [25].

Total RNA isolation and reverse-transcription quantitative polymerase chain reaction (RT-qPCR)

Total RNA was isolated from tissues and cultured cells using the TRIzol Reagent (Thermo Fisher, #15596026), according to the manufacturer's protocol. Equal amounts (1 μg) of total RNA of each sample were subjected to synthesize the first strand cDNA using the PrimeScript™ 1st Strand cDNA Synthesis Kit (Takara, #6110A). The generated cDNA was applied to RT-qPCR analyses using the SYBR® Green Master Mix (Takara, #RR420). Each sample was performed in triplicate. The primers used in this study were listed in Table S2. Raw data were analyzed, and the relative expression levels of genes were normalized to β-Actin according to the $2^{-\Delta\Delta Ct}$ method.

Western blotting and quantification

Tissues and cultured cells were lysed in a 1 × radioimmunoprecipitation assay (RIPA) buffer (Thermo Fisher, #89900) supplemented with the protease inhibitor cocktail (Thermo Fisher, #78429). For each sample, 50 μg of cell lysates was loaded into the SDS-PAGE gel. After membrane transfer and blocking, the protein-bound membranes were probed with primary antibodies, including anti-AF1Q (Abcam, Shanghai, China, #ab109016), anti-TCF4 (Abcam, #ab21-7668), anti-Myc (Sigma-Aldrich, #SAB4301-136), anti-Flag (Sigma-Aldrich, #F1804), and anti-GAPDH (Abcam, #ab8245). The membranes were washed five times with phosphate-buffered saline-Tween 20 buffer, followed by probing with secondary antibodies (Abcam, mouse, #ab205719, and rabbit, #ab205718) and detecting with an ECL detection reagent (Takara, #T710B). The protein signals were quantified using the Image J software, and the relative protein levels of each protein were normalized to the corresponding loading control.

Cell proliferation and cell invasion

The same amounts (approximately 1×10^3) of different cells were seeded into 48-well plates and cultured at 37°C for five days. The cells were collected at a one-day interval and subjected to determine cell proliferation using an MTT kit (Sigma-Aldrich, #11465007001), following the manufacturer's guidelines. Cell invasion was determined using a Boyden chamber assay (Sigma-Aldrich, #ECM550). Briefly, the same amounts (approximately 300) of cells were suspended in serum-free DMEM medium, followed by loading into the upper chambers. The lower chambers were supplemented with a 10% FBS-containing DMEM medium. The whole chambers were placed at a 37°C incubator, and the cells were grown for 24 h. The cells in the lower chambers were fixed using 4% paraformaldehyde (Sigma-Aldrich, #P6148), stained with 0.1% crystal violet (Sigma-Aldrich, #V5265), and photographed using a Nikon Eclipse E200 Hematology Microscope. The crystal violet-positive cells were counted using Image J software.

ChIP assay

Three dishes (100 mm) of Control-KD, AF1Q-KD (#1 and #2), and TCF4-KD (#1 and #2) cells in both MG63 and U2OS backgrounds were fixed 15 min using 1% paraformaldehyde, followed by the addition of 1 M glycine to terminate the reaction. The cells were sonicated for 20 × 30 s with 30 s breaks on ice in a 2 mL lysis buffer (0.1% SDS, 1 mM DTT, 100 mM NaCl, 40 mM Tris-pH 7.8, 3 mM EDTA) containing a 1 × protease inhibitor cocktail. The sonicated cells were subjected to ChIP assay with a kit (Sigma-Aldrich, #17-295) according to the method provided by the manufacturer. The enriched DNA was applied to RT-qPCR analysis with the following primers: forward, 5'-TGAGGAGAATTTA-CCTTTCCCG-3', and reverse, 5'-GCAGCACATA-CATACATAGCT-3'. The relative enrichment was determined using the $2^{-\Delta\Delta Ct}$ method in which $\Delta Ct = Ct_{output}-Ct_{input}$.

Immunohistochemistry (IHC)

Three independent biopsies from patients with each stage of osteosarcoma were used for IHC staining assay according to a previous method [26]. The slides containing sliced tissues were successively probed with anti-AF1Q (1:300 dilution) and biotinylated secondary antibody (Abcam, #ab201485), followed by staining with a Vectastain Avidin-Biotin Complex Kit (Thermo Fisher, #32020) and a DAB peroxidase substrate kit (Abcam, #ab64238), respectively. Pictures were taken using a Nikon Eclipse E200 Hematology Microscope.

Luciferase activity assay

Cells co-expressing pGL4-pCOX2^{WT} + Renilla or pGL4-pCOX2^{Mut} + Renilla were used to determine luciferase activity with the Dual-Luciferase Reporter Assay System (Promega, #E1910) following the manufacturer's guidelines. The relative luciferase activity was determined by normalizing firefly luciferase to Renilla.

IP, mass spectrometry, and Co-IP assays

The U2OS cells were lysed in 1 × RIPA buffer containing a protease inhibitor cocktail, and the cell lysates underwent IP assay using anti-AF1Q (or IgG)-coupled Protein-A beads. After incubating at 4°C for 4 h, the enriched AF1Q (or IgG)-associated complex was washed five times with a 1 × RIPA buffer, followed by resolving in SDS-PAGE gel and incubating with the Proteo-Silver Stain Kit (Sigma-Aldrich, #PROTSIL1). The visualized protein bands were sliced into approximately 5-mm pieces, digested with a Trypsin kit (Promega, #VA1060), and analyzed by mass spectrometry. For the Co-IP assay, the cells were co-transfected with pCDNA3-Flag + pCDNA3-Myc, pCDNA3-Flag + pCDNA3-Myc-TCF4, pCDNA3-Flag-AF1Q + pCDNA3-Myc, and pCDNA3-Flag-AF1Q + pCDNA3-Myc-TCF4, respectively. The cells were lysed in a 1 × RIPA buffer containing a protease inhibitor cocktail, and the cell lysates were incubated with Flag-agarose resin (Sigma-Aldrich, #A4596) and MYC-agarose resin (Sigma-Aldrich, #A7470), respectively. The input and output proteins were applied to immunoblots using anti-Flag and anti-MYC antibodies.

In vitro AlphaScreen

The pGEX-6P-1-AF1Q and pET28a-TCF4 plasmids were transformed into BL21 competent cells. The GST-AF1Q and His-TCF4 proteins were purified using Glutathione Sepharose 4B (GE15-0756-05) and Ni-NTA Agarose (QIAGEN, Shanghai, China, #30210), respectively. The eluted GST-AF1Q and His-TCF4 proteins were used to set up an AlphaScreen system, which consisted of GST-AF1Q (10 μL), His-TCF4 (10 μL), 5 μL glutathione donor beads (PerkinElmer, Waltham, MA, USA, #6762011), 5 μL nickel acceptor beads (PerkinElmer, #6760001), 2 μL naturally derived small molecules from a pool used previously [27], and 3 μL PBS. After thorough mixing, the reaction solution was placed at 25°C for 1.5 h, and the plates were read with an AgileReader (ACTGene Inc., Piscataway, NJ, USA, #1215D29).

PSM0537 treatment in vitro

Cells with 80% confluency were rinsed three times with cold PBS buffer and further cultured in a DMEM medium containing 0, 100, 200, and 400 nM PSM0537 for 12 h. The cells were harvested and underwent RNA and protein analyses.

Tumor xenograft model

Different cells, including MG63/U2OS-Control-KD, MG63/U2OS-AF1Q-KD (#1 and #2), MG63/U2OS-TCF4-KD (#1 and #2), and MG63/U2OS-

COX2-KD (#1 and #2), were cultured to 80% confluency. The cell suspension (100 μL) was injected subcutaneously into eight-week-old C57BL/6 mice (n = 20 for each cell line). Tumor volumes were determined by measuring their length and width and calculated using the following formula: volume = (length × width^2)/2. For the administration of PSM0537, mice injected with osteosarcoma cell suspension were injected with 0, 0.5, 1, and 2 mg/kg PSM0537 at a five-day interval. The tumor volumes were also determined at a five-day interval. All experimental procedures followed a protocol approved by the Institutional Animal Care and Use Committee of Honghui Hospital in Xi'an Jiao Tong University.

Statistical analysis

All experiments were repeated independently in triplicate. For the RT-qPCR analysis, each independent experiment contained three replicates. Data were analyzed using the Statistical Package for Social Sciences software (version 26, IBM, USA) and expressed as the mean ± standard deviation (SD). Statistical significance was defined as $P < 0.05$ (*), $P < 0.01$ (**), and $P < 0.001$ (***).

Results

AF1Q served as an oncogene in osteosarcoma cells and biopsies

AF1Q functions as an oncogene in several cancer types [5-9]. To examine whether AF1Q was also overexpressed in osteosarcoma cells, we first measured its mRNA level in one osteoblast cell line hFOB1.19 and six osteosarcoma cell lines, including MG63, KHOS, 143B, HOS, Saos2, and U2OS. We observed a varying increase in the *AF1Q* mRNA level in osteosarcoma cell lines compared with that in hFOB1.19 cells (**Figure 1A**). Among them, U2OS cells had the most significant increase (5-fold) in the *AF1Q* mRNA level, followed by Saos2 (4.3-fold), MG63 (3.8-fold), HOS (2.8-fold), 143B (2.5-fold), and KHOS (2.1-fold) (**Figure 1A**). We also examined the AF1Q protein level in the same cell lines. Consistent with its mRNA level, AF1Q was accumulated in the osteosarcoma cell lines compared with the hFOB1.19 cells (**Figure 1B** and **1C**). Using biopsies from healthy controls (n = 5) and osteosarcoma patients under different stages (n = 7 for each stage), we compared the *AF1Q* mRNA level and found that it gradually increased with the severity of tumor malignancy (**Figure 1D**). We also equally mixed the homogenates of three representative biopsies from each group and then examined the AF1Q protein level. The results indicated that the AF1Q protein level also gradually increased with the tumor grade (**Figure 1E** and **1F**). Using the same tissue samples, we performed an IHC staining assay and observed the accumulation of AF1Q in cancerous biopsies (**Figure 1G**). Therefore, we conclude that AF1Q also functions as an oncogene in osteosarcoma cells and biopsies and that its expression level is associated with tumor malignancy.

Knockdown of AF1Q significantly inhibited cell proliferation and invasion

Previous studies have shown that AF1Q can affect tumor cell proliferation and invasion [5-9]. To investigate whether it had similar effects on cell proliferation and invasion in osteosarcoma cells, we generated two stable cell lines with *AF1Q* knockdown in both MG63 and U2OS backgrounds. We performed RT-qPCR and western blotting assays to examine the mRNA and protein levels of AF1Q in these cells to verify the successful downregulation of AF1Q (**Figure 2A-D**). Using these cells, cell proliferation was determined through MTT assay. The results showed that the knockdown of *AF1Q* in both MG63 and U2OS backgrounds significantly decreased cell proliferation compared with the control-KD cell lines (**Figure 2E**). No obvious difference was observed when cell proliferation was compared among these four AF1Q-KD cell lines (**Figure 2E**). The Boyden chamber assay results indicated that the knockdown of *AF1Q* dramatically suppressed tumor cell invasion (**Figures 2F** and S1).

COX2 was a target gene of AF1Q

To explore the AF1Q downstream targets involved in cell proliferation and invasion, a microarray analysis was conducted using hFOB1.19, MG63/U2OS-control-KD, and MG63/U2OS-AF1Q-KD cells. After analyzing the microarray results among different cell lines, we found 28 genes whose expression levels were completely reversed in the AF1Q-KD cells compared to that in the Control-KD cells (**Figure 3A** and Table S3). Among these genes, several genes were associated with tumorigenesis: *COX2*, cell

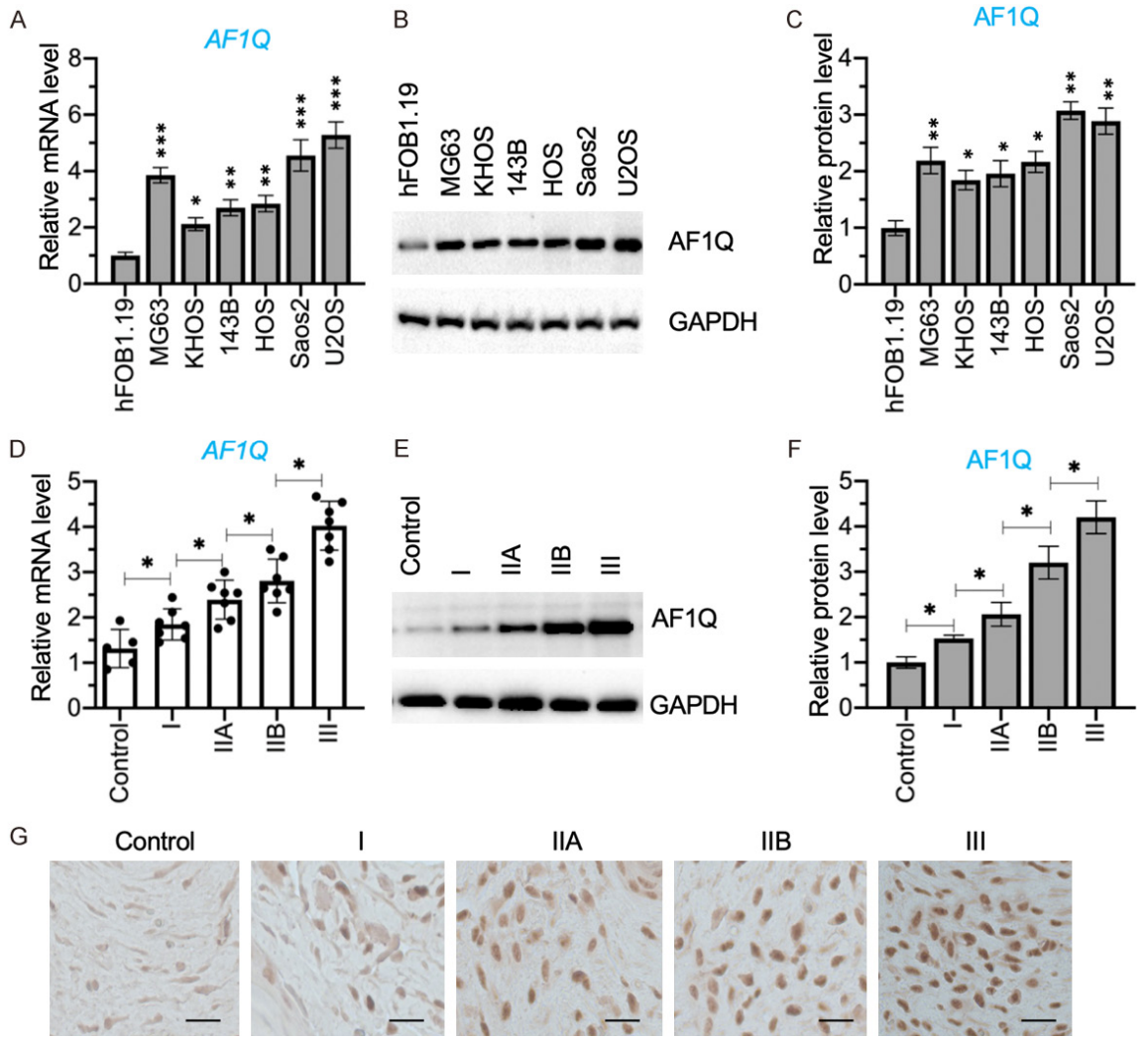

Figure 1. AF1Q was overexpressed in osteosarcoma cells and biopsies (A) AF1Q mRNA level in osteosarcoma cells. Total RNA samples from hFOB1.19, MG63, KHOS, 143B, HOS, Saos2, and U2OS cells were subjected to RT-qPCR analysis to examine the AF1Q mRNA level. *P < 0.05, **P < 0.01, and **P < 0.001. (B and C) The AF1Q protein level in osteosarcoma cells. Cell lysates in cells shown in (A) were subjected to western blotting to examine the AF1Q and GAPDH (loading control) protein levels (B). The intensity of protein bands was quantified and normalized to GAPDH (C). *P < 0.05, **P < 0.01, and **P < 0.001. (D) The AF1Q mRNA level in osteosarcoma biopsies. Total RNA from the controls (tissues adjacent to femurs collected from uncancerous patients with femur fracture) (n = 5) and osteosarcoma biopsies under different TNM stages (n = 7 for each TNM stage) were subjected to RT-qPCR analysis to examine the *AF1Q* mRNA level. *P < 0.05. (E and F) The AF1Q protein level in osteosarcoma biopsies. Tissue homogenate mixtures from three representative samples showing in (D) were subjected to western blotting to examine the AF1Q and GAPDH (loading control) protein levels (E). The intensity of the protein bands was quantified and normalized to GAPDH (F). *P < 0.05. (G) IHC staining results. One representative biopsy from each group showing in (D) was subjected to IHC staining by probing with anti-AF1Q. Bars = 50 μm.

division cycle 25 (*CDC25*), baculoviral IAP repeat containing 5 (*BIRC5*), BCL2 associate X (*BAX*), and BCL2 interacting mediator of cell death (*BIM*) (**Figure 3A** and Table S3). *COX2*, *CDC25*, and *BIRC5* were downregulated, whereas *BAX* and *BIM* were upregulated in AF1Q-KD cells (**Figure 3A** and Table S3). To verify whether these differentially expressed genes were dependent on *AF1Q* expression, RT-qPCR analyses were performed to examine their expression in AF1Q-KD cells. The results indicated that the knockdown of *AF1Q* in both MG63 and U2OS cells caused a significant deduction of *CDC25* (**Figure 3B**), *BIRC5* (**Figure 3C**), and *COX2* (**Figure 3D**). By contrast, the knockdown of *AF1Q* resulted in the upregulation of *BAX*

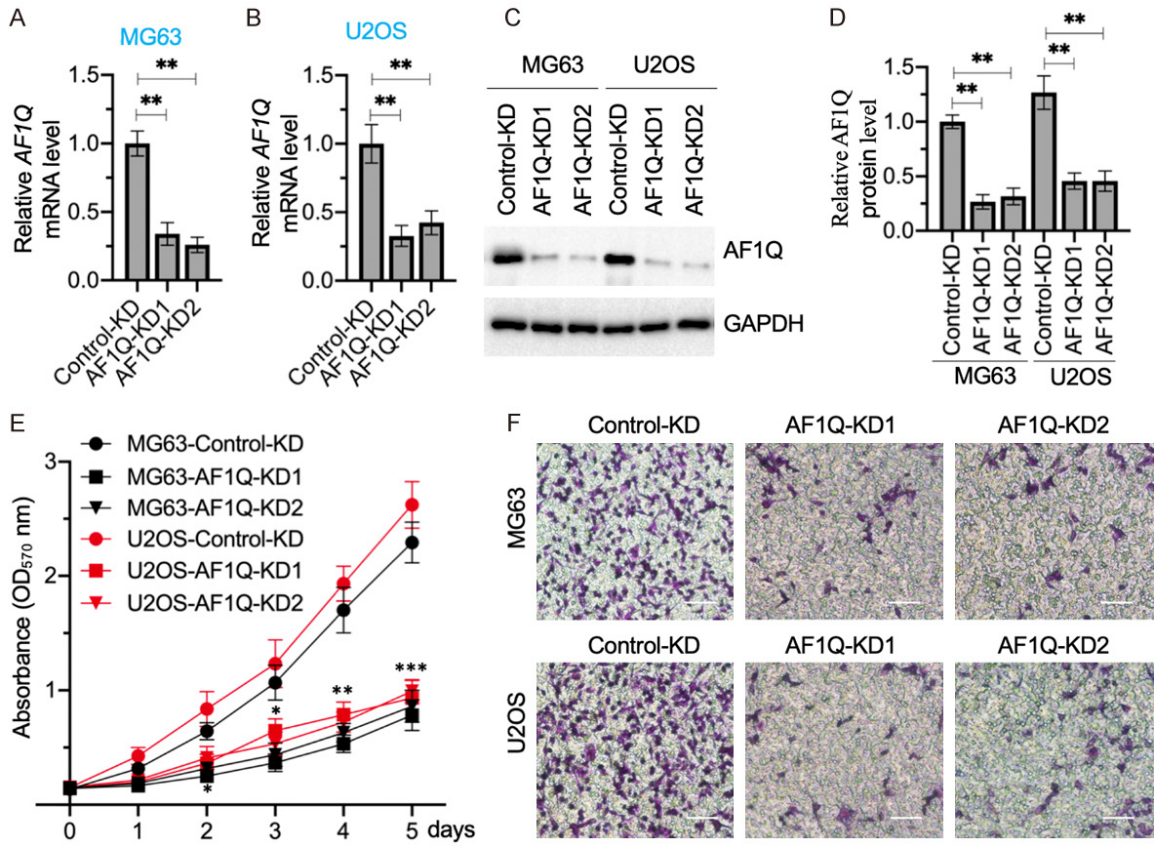

Figure 2. Knockdown of *AF1Q* decreased cell proliferation and invasion. (A and B) The *AF1Q* mRNA level. Total RNA samples from Control-KD and AF1Q-KD (#1 and #2) in both MG63 (A) and U2OS (B) backgrounds were subjected to RT-qPCR analysis to examine the *AF1Q* mRNA level. $^{**}P < 0.01$. (C and D) The AF1Q protein level. Cell lysates in cells shown in (A and B) were subjected to Western blotting to examine the AF1Q and GAPDH (loading control) protein levels (C). The intensity of protein bands was quantified and normalized to GAPDH (D). $^{**}P < 0.01$. (E) Cell proliferation results. Cells shown in (A and B) were subjected to determine cell proliferation using the MTT method at different time points. $^{*}P < 0.05$, $^{**}P < 0.01$, and $^{**}P < 0.001$. (F) Cell invasion results. Cells shown in (A and B) were subjected to the Boyden chamber assay, and the invaded cells were stained using 0.1% crystal violet. Bars = 100 μm.

(**Figure 3E**), *BIM* (**Figure 3F**), and TATA element modulatory factor 1 (*TMF1*) (**Figure 3G**). Owing to the importance of *COX2* in cell proliferation and invasion, we only focused on how AF1Q regulates the *COX2* expression in succeeding studies.

AF1Q assembled a complex with TCF4 to control the COX2 expression

AF1Q has been shown to function as a cofactor of transcription factors [12]. To dissect the AF1Q-associated transcriptional complex in osteosarcoma cells, IP assays were performed using anti-AF1Q (or IgG)-coupled protein-A beads in the homogenate mixture of three cancerous biopsies from stage III osteosarcoma patients. The purified protein complexes underwent silver staining (**Figure 4A**) and mass spectrometry. A total of 42 AF1Q-assocaited proteins were identified (Table S4). Only one transcription factor, TCF4, was found in analyzing the candidates. A previous study showed that AF1Q could directly interact with TCF7, a member of the TCF transcription factor family. Thus, we speculated that AF1Q could also directly interact with TCF4. To verify this hypothesis, IP assays were performed using anti-AF1Q (or IgG)-coupled protein-A beads in U2OS cell lysates. The immunoprecipitated protein complexes were examined to determine whether AF1Q could pull down TCF4. As expected, TCF4 was found in the AF1Q-immunoprecipated complex but not in the IgG-immunoprecipitated complex (**Figure 4B**). To further verify the direct interaction between AF1Q and TCF4, crossed-

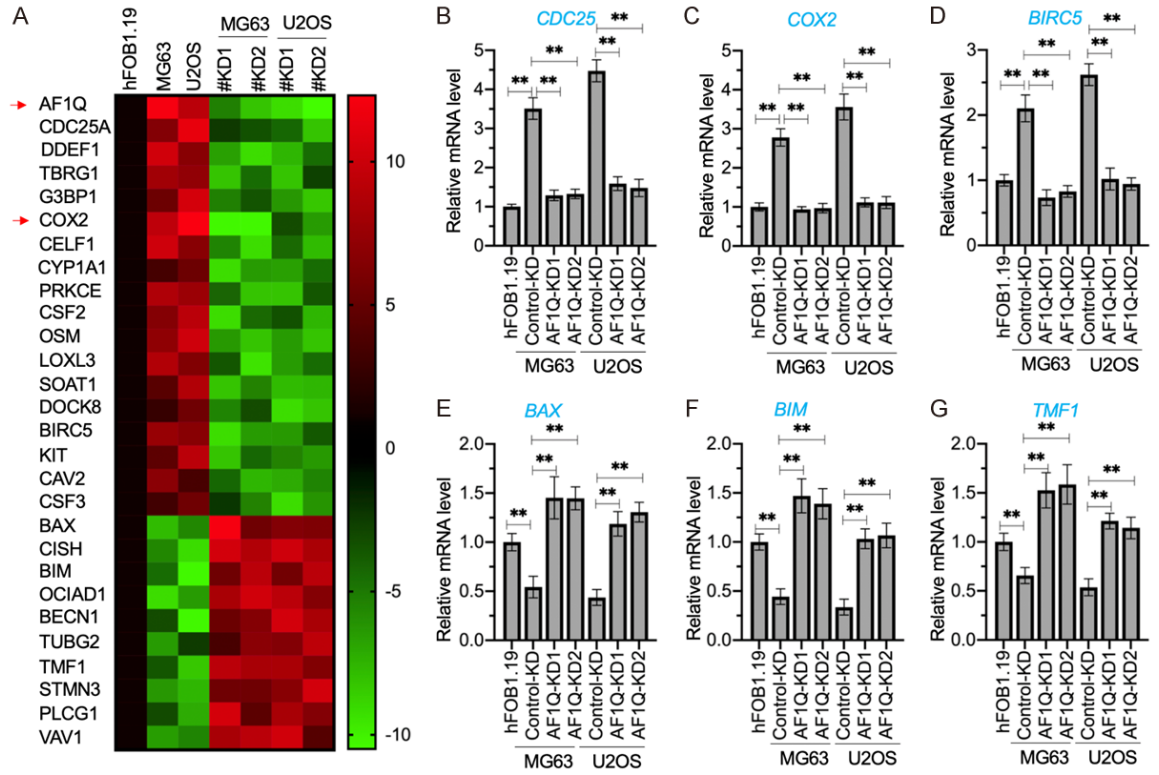

Figure 3. Identification of AF1Q-dependent genes and verification of their expression by RT-qPCR. (A) Microarray results. The total RNA samples from hFOB1.19, Control-KD and AF1Q-KD (#1 and #2) in both MG63 and U2OS backgrounds were subjected to a microarray assay. The differentially expressed genes were shown by a heatmap. *AF1Q* and *COX2* are indicated by red arrows. (B-G) RT-qPCR results. The total RNA samples from hFOB1.19, Control-KD, and AF1Q-KD (#1 and #2) in both MG63 and U2OS backgrounds were subjected to RT-qPCR to examine the mRNA levels of *CDC25* (B), *COX2* (C), *BIRC5* (D), *BAX* (E), *BIM* (F), and *TMF1* (G). $^{**}P < 0.01$.

Co-IP assay was conducted on cells expressing Flag-AF1Q and Myc-TCF4. The Co-IP assay results showed that AF1Q and TCF4 could pull down each other (**Figure 4C**), suggesting that they could interact directly. To determine whether *COX2* was also a target gene of TCF4 in osteosarcoma cells, we generated *TCF4* knockdown cells and examined their effect on *COX2* expression. The RT-qPCR results indicated that *COX2* was downregulated following the knockdown of *TCF4* (**Figure 4D**). Using the same cell lines, we also examined both TCF4 and COX2 protein levels. The immunoblots showed that the COX2 protein level was decreased with the suppression of TCF4 (**Figure 4E** and **4F**).

To determine whether *COX2* was a direct target of TCF4, we searched for the binding site of TCF4 in the promoter of *COX2* using the TCF4 consensus sequence (A-C/G-A/T-T-C-A-A-A-G). A potential TCF4 binding site (AGCTACAAAG) localized between (-636) and (-645) of the *COX2* ATG site was identified (Figure S2A). The wild-type (WT) promoter of *COX2* and the mutated promoter (changing AGCTACAAAG to TAATACCCCA) were constructed into a luciferase vector, respectively (Figure S2A). The luciferase assay results showed that the knockdown and overexpression of *TCF4* caused a decrease and increase in luciferase activities in the WT promoter, respectively (Figure S2B). By contrast, the knockdown and overexpression of *TCF4* did not change the luciferase activities (Figure S2B). These results suggest that TCF4 bound to the promoter of *COX2* through the AGCTACAAAG site. ChIP assays were also performed using anti-TCF4, anti-AF1Q, and IgG in MG63/U2OS-control-KD, MG63/U2OS-AF1Q-KD, and MG63/U2OS-TCF4-KD cells. The results showed that the occupancies of both TCF4 and AF1Q on the promoter of *COX2* were significantly decreased in MG63/U2OS-TCF4-KD cells compared with MG63/U2OS-control-

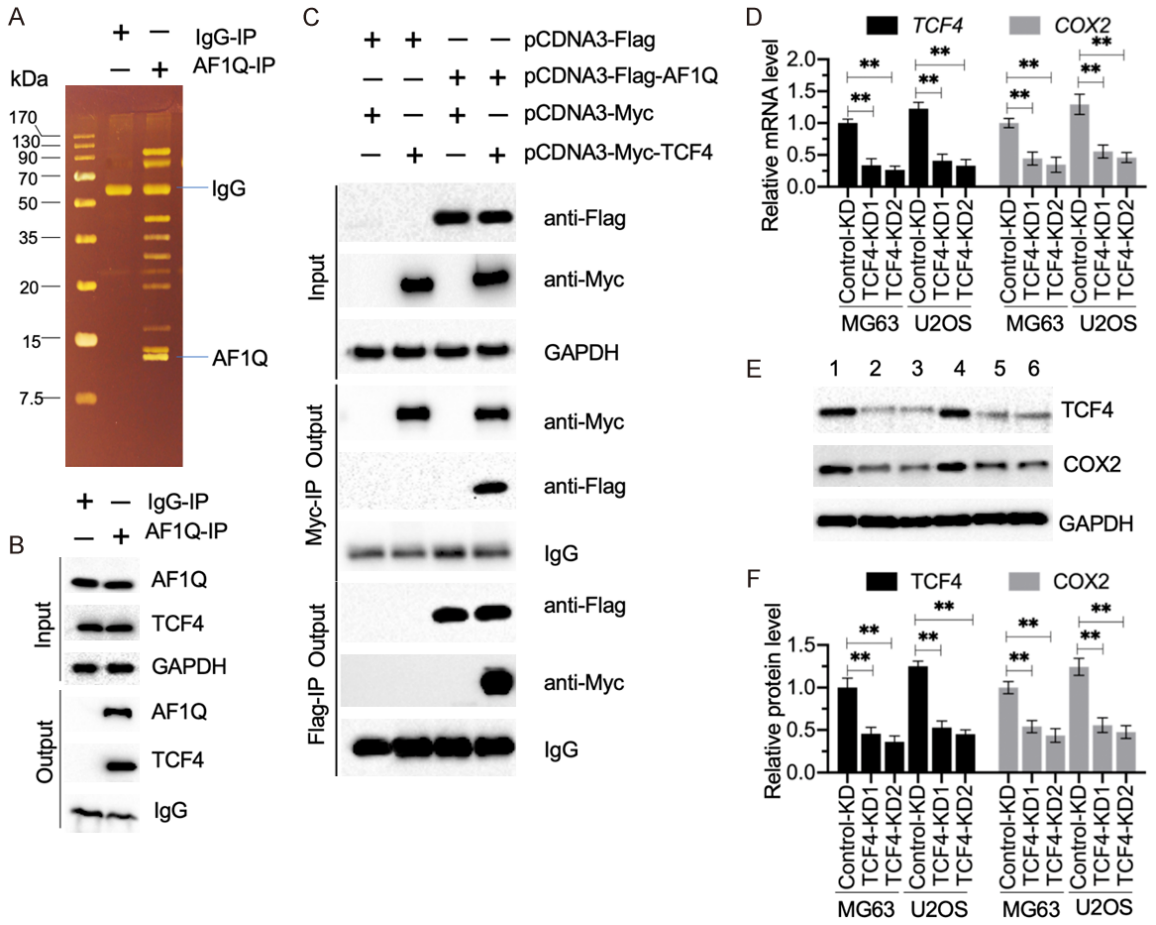

Figure 4. AF1Q assembled a complex with TCF4 in *vitro* and *in vivo*. (A) Silver staining result. The homogenate mixtures of three cancerous biopsies from stage III osteosarcoma patients were subjected to IP assays using anti-AF1Q (or IgG)-coupled protein-A beads. The purified protein complexes were used for silver staining, and the IgG and AF1Q bands were indicated. (B) AF1Q assembled a complex with TCF4 *in vivo*. The U2OS cell lysates were used for IP assays with anti-AF1Q (or IgG)-coupled protein-A beads. The input and output proteins were subjected to western blotting to examine the AF1Q and TCF4 protein levels. GAPDH and IgG were the loading controls of the input and output, respectively. (C) AF1Q interacted with TCF4 directly. MG63 cells expressing different combinations, as shown in the figure, were lysed and subjected to IP assays with Flag- and Myc-agarose. The input and output proteins were subjected to western blotting with anti-Flag and anti-Myc antibodies. GAPDH and IgG were the loading controls of the input and output, respectively. (D) The mRNA levels of *TCF4* and *COX2*. The total RNA samples from Control-KD and TCF4-KD (#1 and #2) in both MG63 and U2OS backgrounds were subjected to RT-qPCR to examine the mRNA levels of *TCF4* and *COX2*. $^{**}P < 0.01$. (E and F) Protein levels of TCF4 and COX2. The cells used in (D) were subjected to western blotting to examine the protein levels of TCF4, COX2, and GAPDH (loading control) (E). 1: Control-KD in MG63 background; 2: TCF4-KD1 in MG63 background; 3: TCF4-KD2 in MG63 background; 4: Control-KD in U2OS background; 5: TCF4-KD1 in U2OS background; 6: TCF4-KD2 in U2OS background. The intensity of the protein bands was quantified and normalized to GAPDH (F). $^{**}P < 0.01$.

KD cells (Figure S2C). We observed only a slight decrease in TCF4 occupancy but a significant deduction of AF1Q occupancy in the promoter of *COX2* in MG63/U2OS-AF1Q-KD cells compared with MG63/U2OS-control-KD cells (Figure S2D). These results suggest that the AF1Q occupancy in the promoter of *COX2* was dependent on TCF4 and that AF1Q could promote the binding of TCF4.

Knockdown of either TCF4 or COX2 could decrease cell proliferation and invasion

The above results showed that the knockdown of *AF1Q* decreased osteosarcoma cell proliferation and invasion. Similarly, we also generated *COX2* knockdown cells (Figure S3) and examined cell proliferation and invasion in both COX2-KD and TCF4-KD cells. The MTT results

in MG63/U2OS-control-KD and MG63/U2OS-TCF4-KD cells showed that the knockdown of *TCF4* in both MG63 and U2OS backgrounds significantly decreased cell proliferation (Figure S4A). The Boyden chamber assay results showed that the knockdown of *TCF4* dramatically decreased the ability of cell invasion (Figure S4B and S4C). The knockdown of *COX2* in both the MG63 and U2OS backgrounds significantly decreased cell proliferation (Figure S4D) and cell invasion (Figure S4E and S4F).

Knockdown of AF1Q, TCF4, or COX2 decreased tumor growth and metastasis in vivo

The significant *in vitro* effects of the knockdown of *AF1Q, TCF4, or COX2* on cell proliferation and invasion motivated us to determine the *in vivo* effects. Accordingly, we injected the cell suspension of MG63/U2OS-control-KD, MG63/U2OS-AF1Q-KD, MG63/U2OS-TCF4-KD, and MG63/U2OS-COX2-KD cells into mice. We observed that the tumor volumes were markedly decreased in the MG63/U2OS-AF1Q-KD (**Figure 5A**), MG63/U2OS-TCF4-KD (**Figure 5B**), and MG63/U2OS-COX2-KD cells (**Figure 5C**) compared with MG63/U2OS-control-KD. In addition, we also determined tumor volumes in the lungs, the most common metastatic site of osteosarcoma spreading. Similarly, we found that the knockdown of *AF1Q*, *TCF4,* or *COX2* decreased metastasis in the lungs (**Figure 5D-F**). These results suggest that targeting *AF1Q*, *TCF4,* or *COX2* in osteosarcoma may prevent tumor cell growth.

Screening small molecules that disrupt the AF1Q-TCF4 interaction

Our laboratory has established a compound pool that collects nearly 20,000 chemical compounds derived from plants and marine species [27]. Using this compound pool, we successfully screened several small molecules that target C-terminal binding protein 2-histone acetyltransferase p300 and tumor necrosis factor receptor type 1-associated DEATH domain protein-TNF receptor 2 interactions. Thus, we were also interested in screening small molecules that disrupted the AF1Q-TCF4 interaction using the same compound pool. For this purpose, we expressed, purified, and eluted GST-AF1Q and His-TCF4 proteins and then bound these two proteins to the donor beads and acceptor beads in the AlphaScreen system (**Figure 6A**). Using different concentrations of GST-AF1Q (0, 40, 80, 120, 160, 200, 240, 280, and 320 nM) and His-TCF4 (10, 20, 40, 80, 160, and 320 nM), AlphaScreen signals were detected to determine the optimal protein concentrations for screening. The results showed that the AlphaScreen signals reached saturation when the concentrations of GST-AF1Q were higher than 160 nM and the concentrations of His-TCF4 were higher than 40 nM (**Figure 6B**). Thus, we used 160 nM GST-AF1Q and 40 nM His-TCF4 for high-throughput screening. Fortunately, we obtained a small molecule numbered PSM0537 (**Figure 6C**), which significantly decreased the AlphaScreen signal to less than 5,000. The half-maximal inhibitory concentration (IC_{50}) of PSM0537 was determined and found to exhibit a strong potential to disrupt the AF1Q-TCF4 binding with IC_{50} = 210.3 ± 15.6 nM (**Figure 6D**). To further solidify this conclusion, we used a series of concentrations of PSM0537 (0, 50, 100, 200, and 400 nM) to inhibit the AF1Q-TCF4 binding. The results indicated that 50, 100, 200, and 400 nM PSM0537 resulted in 25%, 40%, 53%, and 85% inhibition of the AF1Q-TCF4 binding, respectively (**Figure 6E**), suggesting that PSM0537 is a specific inhibitor of the AF1Q-TCF4 interaction.

PSM0537 treatment repressed COX2 expression, inhibited cell proliferation and invasion in vitro, and prevented tumor growth and metastasis in vivo

As PSM0537 could significantly inhibit the AF1Q-TCF4 interaction in the AlphaScreen system, we determined its effect on osteosarcoma cells. By treating U2OS cells with a series of concentrations of PSM0537 (0, 100, 200, and 400 nM), the effects on *AF1Q*, *TCF4*, and *COX2* mRNA levels were examined. The RT-qPCR results showed that PSM0537 treatments did not change the mRNA levels of both *AF1Q* and *TCF4* but caused a dose-dependent decrease in *COX2* mRNA levels (**Figure 7A**). The immunoblots also indicated that PSM0537 treatments did not change the AF1Q and TCF4 protein levels but gradually decreased the COX2 protein level, following the increase in PSM0537 concentrations (**Figure 7B** and **7C**). PSM0537 was designed to disrupt the AF1Q-TCF4 interaction, and thus we were not surprised that it could not change the mRNA and protein levels of AF1Q and TCF4. Using PSM0537-treated

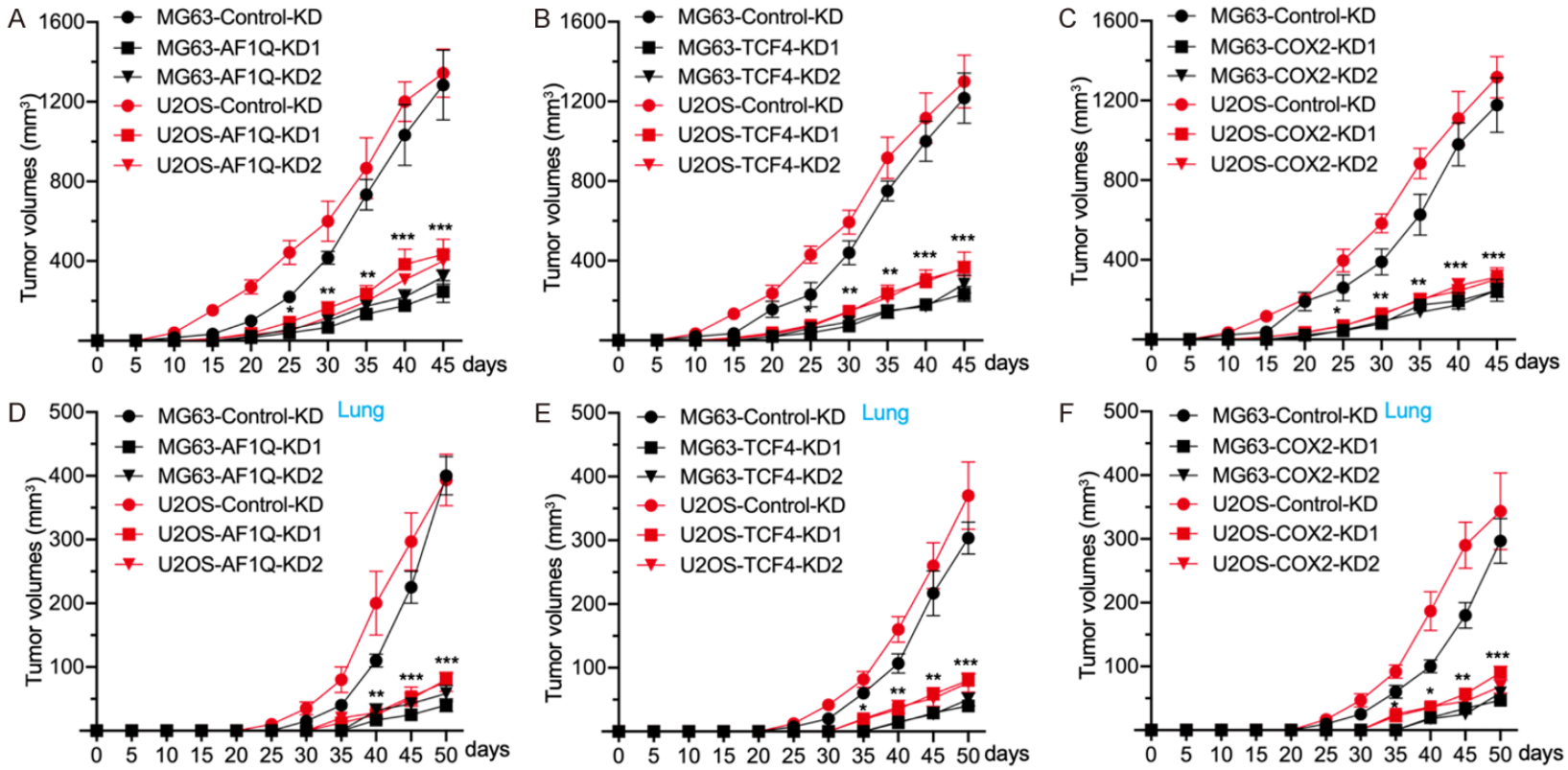

Figure 5. Knockdown of *AF1Q*, *TCF4*, or *COX2* decreased tumor growth and metastasis. (A-C) Tumor volumes of mice injected with AF1Q-KD, TCF4-KD, and COX2-KD cells. The Control-KD, AF1Q-KD (A), TCF4-KD (B), and COX2-KD (C) cells in both MG63 and U2OS backgrounds were injected into C57BL/6 mice (n = 40 for each group), respectively. The tumor volumes were determined at five-day intervals to 45 days. $*P < 0.05$, $**P < 0.01$, and $***P < 0.001$. (D-F) Tumor volumes in the lungs. At each time point, the mice (n = 3) in each group showing in (A-C) were euthanized with carbon dioxide to determine the tumor volumes in the lungs. $*P < 0.05$, $**P < 0.01$, and $***P < 0.001$.

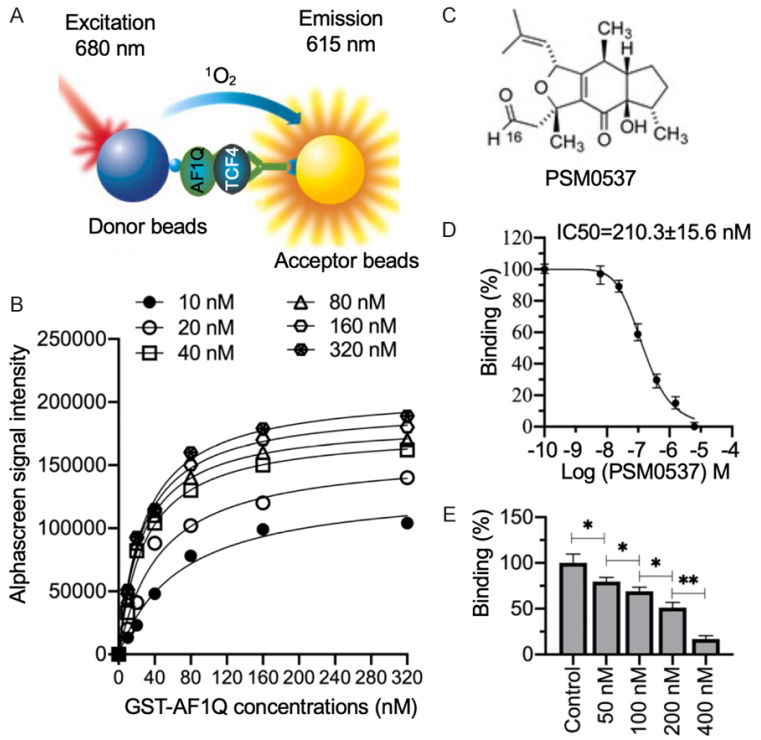

Figure 6. PSM0537 specifically disrupted the AF1Q-TCF4 interaction in the AlphaScreen system. (A) Schematic diagram of the AlphaScreen model binding GST-AF1Q and His-TCF4. (B) Optimal GST-AF1Q and His-TCF4 concentrations for the AlphaScreen assay. A series of concentrations of GST-AF1Q (0, 40, 80, 120, 160, 200, 240, 280, and 320 nM) was mixed with varying concentrations of His-TCF4 (10, 20, 40, 80, 160, and 320 nM) to generate AlphaScreen signals. (C) Chemical structure of PSM0537. (D) IC_{50} of PSM0537. A series of concentrations of PSM0537, as shown in the figure, were mixed with an AlphaScreen reaction containing 160 nM GST-AF1Q and 40 nM His-TCF4 respectively. The IC_{50} of PSM0537 was calculated using Prism 8 software. (E) Verification of the PSM0537 inhibitory efficiency. Different concentrations of PSM0537 (0, 50, 100, 200, and 400 nM) were added to the same AlphaScreen reaction system shown in (D) to determine the inhibitory effects on AF1Q-TCF4 binding. *$P < 0.05$ and ** $P < 0.01$.

U2OS cells, ChIP assays were conducted using anti-TCF4, anti-AF1Q, and IgG. The results showed that the occupancies of both TCF4 and AF1Q were dose-dependently decreased following PSM0537 treatments (Figure S5). The effects of PSM0537 on cell proliferation and invasion were also determined. The MTT assay results showed that PSM0537 treatments caused a dose-dependent decrease in inhibition in cell proliferation (**Figure 7D**). A dose-dependent decrease in invading cell numbers following the treatments of PSM0537 was also observed (**Figure 7E** and **7F**). These results suggest that PSM0537 is also functional in osteosarcoma cells. Moreover, we also examined the cytotoxic effect of PSM0537 on uncancerous hFBOB1.19 cells and evaluated whether PSM0537 treatments could induce apoptosis. Treatments of PSM0537 did not result in morphological changes of both hFOB1.19 and U2OS cells (Figure S6A). The MTT results using hFOB1.19 cells showed that only high dosage (400 nM) of PSM0537 caused a slight decrease in cell proliferation (Figure S6B). The immunoblot results indicated that PSM-0537 treatments could not change the protein levels of apoptotic markers (Caspase-3 and -7) (Figure S6C and S6D).

To determine the *in vivo* effect of PSM0537 on tumor growth and metastasis, we administrated different concentrations of PSM0537 (0.5, 1, and 2 mg/kg) in mice injected with MG63 or U2OS cells. The tumor volumes in the mice injected with both MG63 and U2OS decreased with the increase in PSM0537 concentrations (**Figure 8A** and **8B**). In addition, we determined the tumor volumes in the lungs and observed a similar pattern; that is, the administration of PSM0537 caused a dose-dependent decrease in tumor volumes (**Figure 8C** and **8D**). The 2 mg/kg dose inhibited more than 90% tumor volumes (**Figure 8A-D**).

Discussion

Although AF1Q has been identified to overexpress in leukemia and multiple solid tumors [5-9], its expression level in osteosarcoma cells remains unknown. AF1Q is a transcriptional cofactor, but its associated transcription factors and regulatory genes are still obscure in different cancers [5-9, 12]. In this study, we demonstrate that AF1Q is overexpressed in both osteosarcoma cells and cancerous biopsies. The overexpressed AF1Q interacts with TCF4 to form the AF1Q-TCF4 complex, which binds to the promoter of *COX2* to induce its

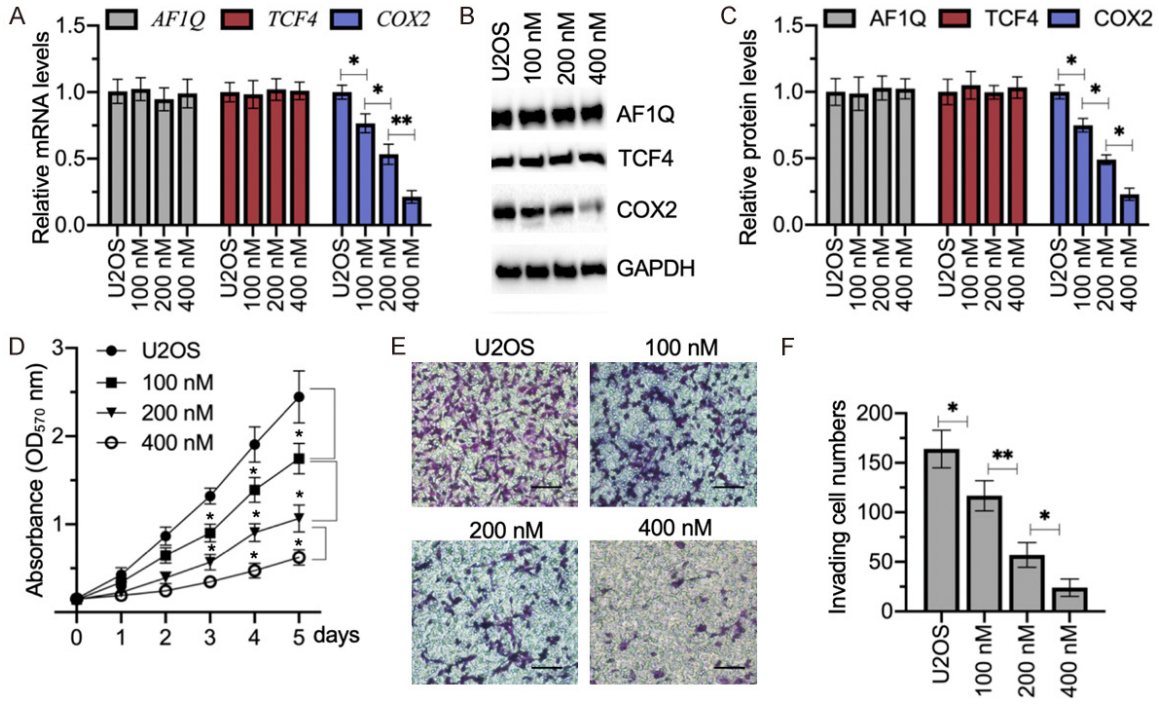

Figure 7. PSM0537 suppressed the expression of *COX2* in osteosarcoma cells and inhibited cell proliferation and invasion. (A) The mRNA levels of *AF1Q*, *TCF4*, and *COX2*. The U2OS cells were treated with different concentrations of PSM0537 (0, 100, 200, and 400 nM), followed by RT-qPCR analyses, to examine the mRNA levels of *AF1Q*, *TCF4*, and *COX2*. **P* < 0.05 and ** *P* < 0.01. (B and C) Protein levels of AF1Q, TCF4, and COX2. The cell lysates in the cells shown in (A) were subjected to western blotting to examine the protein levels of AF1Q, TCF4, COX2, and GAPDH (loading control) (B). The intensity of the protein bands was quantified and normalized to GAPDH (C). ***P* < 0.01. (D) Cell proliferation results. The cells shown in (A) were subjected to determine cell proliferation using the MTT method at different time points. **P* < 0.05. (E and F) Cell invasion results. The cells shown in (A) were subjected to the Boyden chamber assay, and the invaded cells were stained using 0.1% crystal violet (E). The crystal violet-positive cells were counted (F). **P* < 0.05 and ** *P* < 0.01. Bars = 100 μm.

expression (**Figure 9A**). Using the AF1Q-TCF4 interaction as a target, we screen and obtain the compound PSM0537, which disrupts the AF1Q-TCF4 interaction and blocks their binding to the promoter of *COX2*, causing the downregulation of *COX2* and affecting cell proliferation and invasion (**Figure 9B**).

AF1Q overexpression in osteosarcoma cells and in other tumors suggests that AF1Q is an important oncogene. Therefore, targeting AF1Q may be an effective strategy to inhibit tumor cell growth. Using a microarray analysis, we found 28 AF1Q-dependent genes because their expression levels were completely reversed in Control-KD and AF1Q-KD cells (**Figure 3A** and Table S3). Except for *COX2*, two classes of genes, namely the cell cycle gene *CDC25* and apoptotic genes (*BIRC5*, *BAX,* and *BIM*), are also dependent on AF1Q (**Figure 3A** and Table S3). The diversity of these genes suggests that AF1Q may have many downstream targets. Thus, targeting AF1Q alone may cause a broad spectrum of effects. In the present study, we only focused on how AF1Q regulates the expression of *COX2* but not the other AF1Q-dependent genes. To determine the specificity of the AF1Q-TCF4 complex in the regulation of *COX2*, we also examined the expression levels of *CDC25*, *BIRC5*, *BAX,* and *BIM* in TCF4-KD cells. We found that the knockdown of *TCF4* did not change the expression of these four genes (Figure S7), suggesting that the AF1Q-TCF4 complex is only a response to *COX2* expression in osteosarcoma cells. These results also suggest that AF1Q may be associated with other transcription factors to control the expression of other AF1Q-dependent genes. A critical issue in future studies is to reveal the regulatory mechanisms of AF1Q-dependent genes.

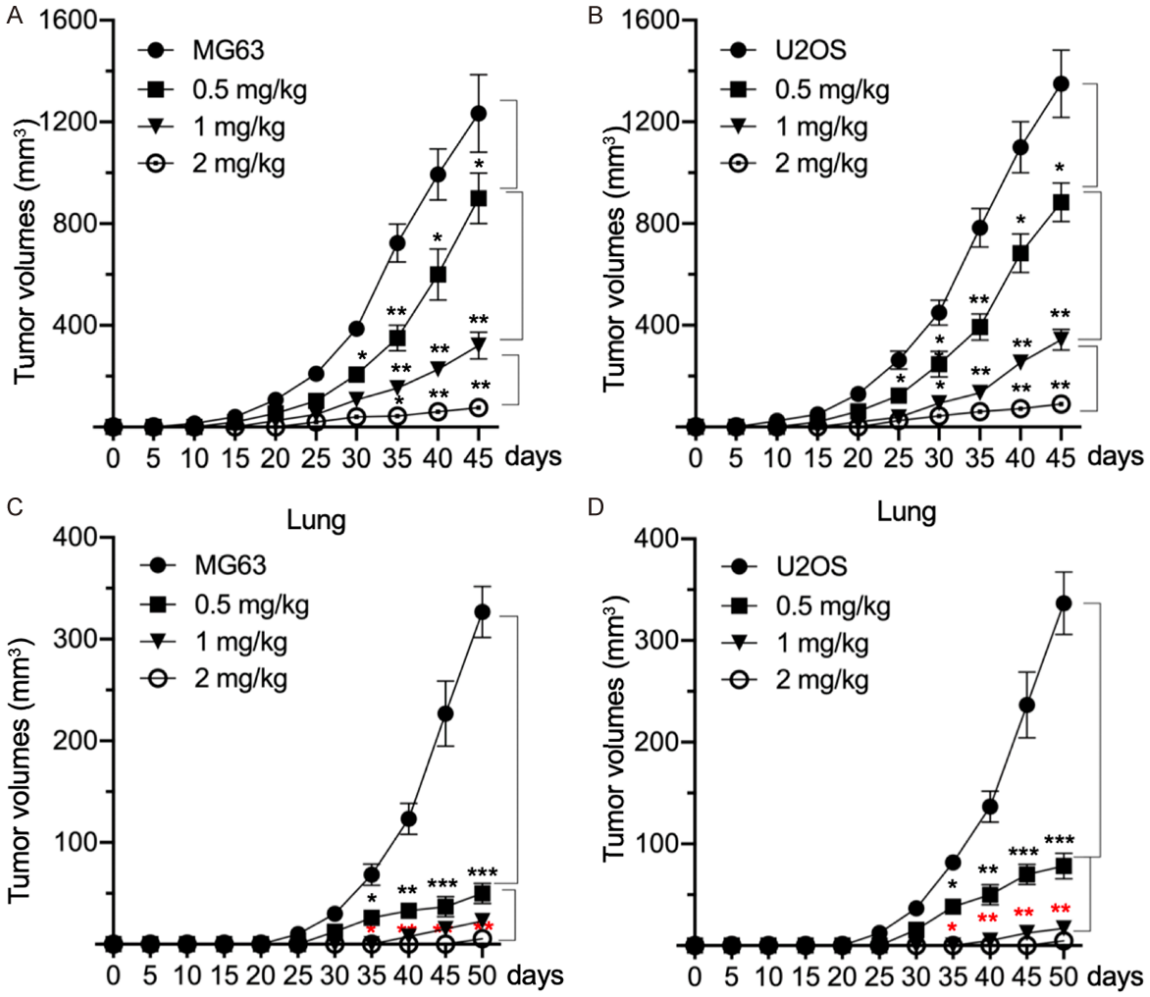

Figure 8. PSM0537 decreased tumor growth and metastasis. (A and B) Effect of PSM0537 on tumor volumes. The MG63 (A) and U2OS (B) cells were injected into C57BL/6 mice, respectively. Different concentrations (0, 0.5, 1, and 2 mg/kg) of PSM0537 were injected into the mice at five-day intervals. Tumor volumes were also determined at five-day intervals to 45 days. *$P < 0.05$ and **$P < 0.01$. (C and D) Tumor volumes in the lungs. At each time point, the mice (n = 3) in each group shown in (A and B) were euthanized with carbon dioxide to determine the tumor volumes in the lungs. *$P < 0.05$, **$P < 0.01$, and ***$P < 0.001$.

COX2 is an important inflammatory factor that contributes to the promotion of cell invasion by mediating epithelial-to-mesenchymal transition and activating the STAT3 pathway [13, 28-30]. In this study, we did not investigate the downstream of COX2 in osteosarcoma cells. More efforts are required to investigate the downstream events of COX2 in future investigations. PSM0537 is obtained by a strategy designed to disrupt the AF1Q-TCF4 interaction. Our results showed that PSM0537 did not change the mRNA and protein levels of both AF1Q and TCF4 but instead impaired their bindings on the promoter of *COX2* (**Figures 7** and S6). As the structure of the AF1Q-TCF4 complex remains unknown, the other important issues for future studies are to investigate how the AF1Q-TCF4 complex is assembled and how PSM0537 disrupts their binding. Moreover, efforts such as the chemical synthesis of active PSM0537 and its modification to obtain more active compounds are also crucial for large-scale clinical trials of this compound. Owing to the conserved role of AF1Q and COX2 in different cancers, there is a high possibility that the AF1Q-TCF4 complex also contributes to the regulation of *COX2* in other cancers. Thus, PSM0537 may also be functional in the suppression of tumor cell growth in other cancer types. The low cytotoxicity of PSM0537 to uncancerous cells sug-

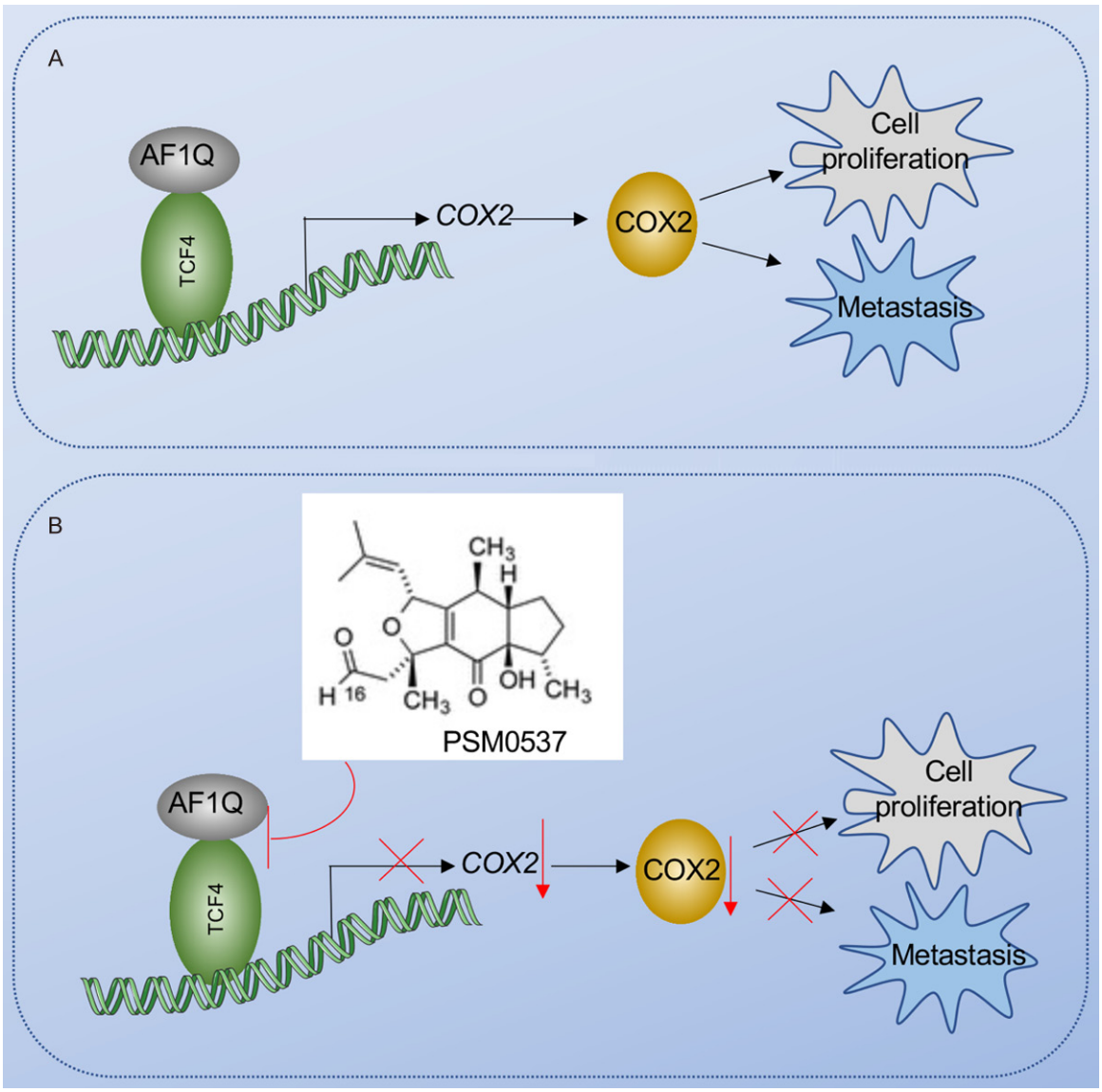

Figure 9. Schematic diagrams of the AF1Q-TCF4 complex and targeting the AF1Q-TCF4 complex with PSM0537 to inhibit osteosarcoma cell growth and metastasis. A. Schematic diagram of the AF1Q-TCF4 complex in osteosarcoma cells. The AF1Q-TCF4 complex docks on the promoter of *COX2* to induce its expression. The accumulated COX2 promotes cell proliferation and metastasis, leading to the tumorigenesis of osteosarcoma. B. Schematic diagram of PSM0537 disrupting the AF1Q-TCF4 complex. PSM0537 specifically disrupts the interaction between AF1Q and TCF4, resulting in a decrease in *COX2* and inhibiting cell proliferation and tumor metastasis.

gests that it may be a promising chemical for chemotherapeutic treatment.

In summary, we demonstrated the overexpression of the AF1Q-TCF4 complex and its target gene *COX2* in osteosarcoma cells and cancerous biopsies. The knockdown of *AF1Q*, *TCF4,* or *COX2* decreased cell proliferation and invasion. Using the AlphaScreen system, we found that PSM0537 could significantly disrupt the AF1Q-TCF4 interaction. The administration of PSM0537 could prevent osteosarcoma cell growth and invasion *in vitro* and inhibit tumor growth and metastasis *in vivo*. Our results may provide a new avenue for the chemotherapy of osteosarcoma.

Acknowledgements

This work was supported by a grant from Natural Science Foundation of Shaanxi Province, China (Grant No. 2020JM-688). All exper-

imental procedures used in this study were performed in accordance with the approved guidelines of the ethical board of Xi'an Jiaotong University College of Medicine.

Disclosure of conflict of interest

None.

Address correspondence to: Dr. Xun Chen, Department of Orthopaedic Surgery, Honghui Hospital, Xi'an Jiaotong University, 76 Nanguo Rd, Beilin District, Xi'an 710054, Shaanxi, China. E-mail: fbbycx@stu.xjtu.edu.cn; Dr. Wei Ma, Department of Orthopaedics, The First Affiliated Hospital of Xi'an Jiaotong University, 277 Yanta W Road, Yanta District, Xi'an 710061, Shaanxi, China. E-mail: wei.ma4020@gmail.com

References

[1] Mirabello L, Troisi RJ and Savage SA. International osteosarcoma incidence patterns in children and adolescents, middle ages and elderly persons. Int J Cancer 2009; 125: 229-234.

[2] Kansara M, Teng MW, Smyth MJ and Thomas DM. Translational biology of osteosarcoma. Nat Rev Cancer 2014; 14: 722-735.

[3] Roessner A, Lohmann C and Jechorek D. Translational cell biology of highly malignant osteosarcoma. Pathol Int 2021; 71: 291-303.

[4] Gianferante DM, Mirabello L and Savage SA. Germline and somatic genetics of osteosarcoma - connecting aetiology, biology and therapy. Nat Rev Endocrinol 2017; 13: 480-491.

[5] Tse W, Meshinchi S, Alonzo TA, Stirewalt DL, Gerbing RB, Woods WG, Appelbaum FR and Radich JP. Elevated expression of the AF1q gene, an MLL fusion partner, is an independent adverse prognostic factor in pediatric acute myeloid leukemia. Blood 2004; 104: 3058-3063.

[6] Hu J, Li G, Liu L, Wang Y, Li X and Gong J. AF1q mediates tumor progression in colorectal cancer by regulating AKT signaling. Int J Mol Sci 2017; 18: 987.

[7] Chang XZ, Li DQ, Hou YF, Wu J, Lu JS, Di GH, Jin W, Ou ZL, Shen ZZ and Shao ZM. Identification of the functional role of AF1Q in the progression of breast cancer. Breast Cancer Res Treat 2008; 111: 65-78.

[8] Tiberio P, Lozneanu L, Angeloni V, Cavadini E, Pinciroli P, Callari M, Carcangiu ML, Lorusso D, Raspagliesi F, Pala V, Daidone MG and Appierto V. Involvement of AF1q/MLLT11 in the progression of ovarian cancer. Oncotarget 2017; 8: 23246-23264.

[9] Skotheim RI, Autio R, Lind GE, Kraggerud SM, Andrews PW, Monni O, Kallioniemi O and Lothe RA. Novel genomic aberrations in testicular germ cell tumors by array-CGH, and associated gene expression changes. Cell Oncol 2006; 28: 315-326.

[10] Zhang H, Ren R, Du J, Sun T, Wang P and Kang P. AF1q contributes to adriamycin-induced podocyte injury by activating wnt/beta-catenin signaling. Kidney Blood Press Res 2017; 42: 794-803.

[11] Park J, Kim S, Joh J, Remick SC, Miller DM, Yan J, Kanaan Z, Chao JH, Krem MM, Basu SK, Hagiwara S, Kenner L, Moriggl R, Bunting KD and Tse W. MLLT11/AF1q boosts oncogenic STAT3 activity through Src-PDGFR tyrosine kinase signaling. Oncotarget 2016; 7: 43960-43973.

[12] Park J, Schlederer M, Schreiber M, Ice R, Merkel O, Bilban M, Hofbauer S, Kim S, Addison J, Zou J, Ji C, Bunting ST, Wang Z, Shoham M, Huang G, Bago-Horvath Z, Gibson LF, Rojanasakul Y, Remick S, Ivanov A, Pugacheva E, Bunting KD, Moriggl R, Kenner L and Tse W. AF1q is a novel TCF7 co-factor which activates CD44 and promotes breast cancer metastasis. Oncotarget 2015; 6: 20697-20710.

[13] Moon H, White AC and Borowsky AD. New insights into the functions of Cox-2 in skin and esophageal malignancies. Exp Mol Med 2020; 52: 538-547.

[14] Wang D and Dubois RN. The role of COX-2 in intestinal inflammation and colorectal cancer. Oncogene 2010; 29: 781-788.

[15] Gupta RA and Dubois RN. Colorectal cancer prevention and treatment by inhibition of cyclooxygenase-2. Nat Rev Cancer 2001; 1: 11-21.

[16] Davila-Gonzalez D, Chang JC and Billiar TR. NO and COX2: dual targeting for aggressive cancers. Proc Natl Acad Sci U S A 2017; 114: 13591-13593.

[17] Chen H, Cai W, Chu ESH, Tang J, Wong CC, Wong SH, Sun W, Liang Q, Fang J, Sun Z and Yu J. Hepatic cyclooxygenase-2 overexpression induced spontaneous hepatocellular carcinoma formation in mice. Oncogene 2017; 36: 4415-4426.

[18] Hill R, Li Y, Tran LM, Dry S, Calvopina JH, Garcia A, Kim C, Wang Y, Donahue TR, Herschman HR and Wu H. Cell intrinsic role of COX-2 in pancreatic cancer development. Mol Cancer Ther 2012; 11: 2127-2137.

[19] Lee EJ, Choi EM, Kim SR, Park JH, Kim H, Ha KS, Kim YM, Kim SS, Choe M, Kim JI and Han JA. Cyclooxygenase-2 promotes cell proliferation, migration and invasion in U2OS human osteosarcoma cells. Exp Mol Med 2007; 39: 469-476.

[20] Hu H, Han T, Zhuo M, Wu LL, Yuan C, Wu L, Lei W, Jiao F and Wang LW. Elevated COX-2 expression promotes angiogenesis through EGFR/p38-MAPK/Sp1-dependent signalling in pancreatic cancer. Sci Rep 2017; 7: 470.
[21] Sheng H, Shao J, Morrow JD, Beauchamp RD and DuBois RN. Modulation of apoptosis and Bcl-2 expression by prostaglandin E2 in human colon cancer cells. Cancer Res 1998; 58: 362-366.
[22] Xu L and Croix BS. Improving VEGF-targeted therapies through inhibition of COX-2/PGE2 signaling. Mol Cell Oncol 2014; 1: e969154.
[23] Wu K, Fukuda K, Xing F, Zhang Y, Sharma S, Liu Y, Chan MD, Zhou X, Qasem SA, Pochampally R, Mo YY and Watabe K. Roles of the cyclooxygenase 2 matrix metalloproteinase 1 pathway in brain metastasis of breast cancer. J Biol Chem 2015; 290: 9842-9854.
[24] Qu L and Liu B. Cyclooxygeanse-2 promotes metastasis in osteosarcoma. Cancer Cell Int 2015; 15: 69.
[25] Zhang W, Duan N, Zhang Q, Song T, Li Z, Chen X and Wang K. The intracellular NADH level regulates atrophic nonunion pathogenesis through the CtBP2-p300-Runx2 transcriptional complex. Int J Biol Sci 2018; 14: 2023-2036.
[26] Jensen K, Krusenstjerna-Hafstrom R, Lohse J, Petersen KH and Derand H. A novel quantitative immunohistochemistry method for precise protein measurements directly in formalin-fixed, paraffin-embedded specimens: analytical performance measuring HER2. Mod Pathol 2017; 30: 180-193.
[27] Chen X, Zhang W, Zhang Q, Song T, Yu Z, Li Z, Duan N and Dang X. NSM00158 specifically disrupts the CtBP2-p300 interaction to reverse CtBP2-mediated transrepression and prevent the occurrence of nonunion. Mol Cells 2020; 43: 517-529.
[28] Koliaraki V, Pallangyo CK, Greten FR and Kollias G. Mesenchymal cells in colon cancer. Gastroenterology 2017; 152: 964-979.
[29] Li A, Chen P, Leng Y and Kang J. Histone deacetylase 6 regulates the immunosuppressive properties of cancer-associated fibroblasts in breast cancer through the STAT3-COX2-dependent pathway. Oncogene 2018; 37: 5952-5966.
[30] Gong J, Xie J, Bedolla R, Rivas P, Chakravarthy D, Freeman JW, Reddick R, Kopetz S, Peterson A, Wang H, Fischer SM and Kumar AP. Combined targeting of STAT3/NF-kappaB/COX-2/EP4 for effective management of pancreatic cancer. Clin Cancer Res 2014; 20: 1259-1273.

Table S1. The basic characteristics of osteosarcoma patients and controls

Participants	Gender (F: female; M: male)	Average ages (years)
Control	3F/2F	26.2 ± 2.1
I	4F/3M	15.6 ± 2.3
IIA	2F/5M	17.4 ± 2.5
IIB	4F/3M	16.4 ± 2.0
III	3F/4F	20.1 ± 3.2

Table S2. Primers used for RT-qPCR to detect gene expression levels

Genes	Forward primer (5'-3')	Reverse primer (5'-3')
AF1Q	GAACTGGATCTGTCGGAG	TCTCCTGGTCTGCTGCAG
CDC25	ATCGGACAGAAAGCTAGGT	TATGTCAGGCAGCCAAGCC
COX2	CAGTAGGTGCATTGGAATC	CTCTGATCTTAAAACTAGT
BIRC5	AACCTCTGGAGGTCATCTC	CAGAGACAACTGCGTCTCT
BAX	AGGATGCGTCCACCAAGAAG	CATGTCAGCTGCCACTCGG
BIM	ACCAAGCAGCCGAAGACCA	GTGCTGGGTCTTGTTGGTT
TMF1	CATGGATAGTATAGACACCT	TATTACAGTGCACTGTTA
TCF4	CCATGTATCAGTGCCTGGCT	CCTACTAGGGTGTACTACA

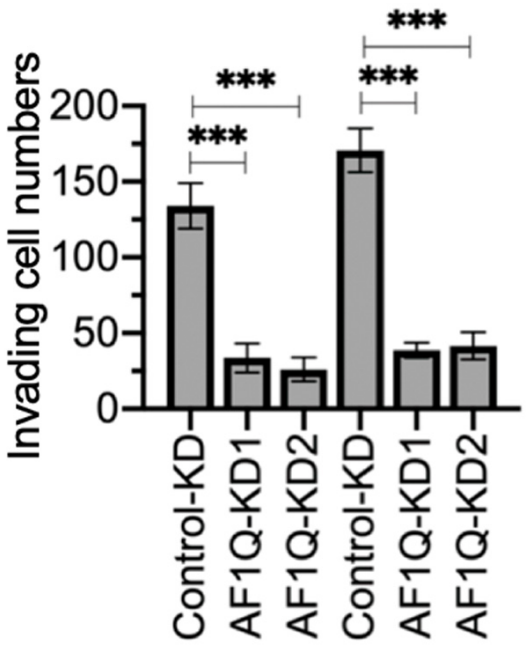

Figure S1. The invading cell numbers of AF1Q-KD cells. The crystal violet-positive cells showing in **Figure 1F** were counted using Image J software. $^{**}P < 0.001$.

Table S3. The AF1Q-dependent genes identified by microarray analysis

Genes	hFOB1.19	MG63	U2OS	MG63-AF1Q-KD1	MG63-AF1Q-KD2	U2OS-AF1Q-KD1	U2OS-AF1Q-KD2
AF1Q	1.0	12.1	9.2	-5.3	-8.2	-9.2	-10.5
CDC25A	1.0	6.4	11.4	-2.4	-3.4	-4.3	-8.2
DDEF1	1.0	10.2	6.7	-6.7	-9.2	-7.6	-4.5
TBRG1	1.0	7.9	7.2	-8.2	-4.5	-8.2	-2.7
G3BP1	1.0	5.3	10.4	-5.3	-3.5	-6.3	-8.3
COX2	1.0	9.4	12.3	-10.3	-10.3	-3.2	-6.5
CELF1	1.0	10.1	6.7	-5.5	-9.2	-4.4	-7.8
CYP1A1	1.0	3.4	5.3	-9.2	-6.5	-6.7	-4.5
PRKCE	1.0	8.6	7.6	-4.2	-8.2	-8.2	-3.6
CSF2	1.0	6.5	9.2	-9.2	-4.4	-3.4	-7.6
OSM	1.0	7.1	10.1	-6.4	-8.2	-6.5	-8.2
LOXL3	1.0	8.7	6.3	-3.6	-9.5	-6.5	-4.5
SOAT1	1.0	4.3	8.7	-8.2	-5.4	-7.8	-7.6
DOCK8	1.0	2.6	5.4	-5.5	-3.2	-9.2	-8.2
BIRC5	1.0	7.4	6.7	-9.2	-6.5	-6.4	-3.7
KIT	1.0	4.6	9.2	-8.2	-4.3	-5.4	-6.4
CAV2	1.0	6.8	3.5	-4.3	-7.6	-7.2	-5.5
CSF3	1.0	3.2	5.4	-2.3	-5.4	-9.2	-6.2
BAX	1.0	-7.8	-5.6	12.1	5.4	6.4	6.2
CISH	1.0	-5.6	-9.1	10.3	8.7	10.1	8.4
BIM	1.0	-4.5	-10.3	5.4	9.2	5.6	9.2
OCIAD1	1.0	-9.2	-6.5	8.3	10.2	9.2	6.5
BECN1	1.0	-3.2	-10.3	5.2	6.5	10.3	8.3
TUBG2	1.0	-6.5	-2.5	3.5	6.8	6.4	9.3
TMF1	1.0	-3.6	-8.3	9.2	8.2	8.3	6.3
STMN3	1.0	-6.3	-7.6	5.4	5.4	6.7	10.3
PLCG1	1.0	-3.1	-7.2	10.4	4.5	8.2	6.4
VAV1	1.0	-6.6	-5.5	8.2	9.2	10.2	4.2

Table S4. The AF1Q-associated proteins identified by MS analysis

Protein	Protein description	Molecular weight (Da)	MASCOT scores
AF1Q	ALL1 Fused Gene From Chromosome 1q	10061	1687
TCF4	Transcription Factor 4	71308	1655
BAD	BCL2 Associated Agonist Of Cell Death	18392	1598
LAMP2	Lysosomal Associated Membrane Protein 2	44961	1545
SRC	SRC Proto-Oncogene, Non-Receptor Tyrosine Kinase	59835	1511
TXNIP	Thioredoxin Interacting Protein	43661	1490
PRDM16	PR/SET Domain 16	140251	1443
DCUN1D1	Defective In Cullin Neddylation 1 Domain Containing 1	30124	1411
NQO1	NAD(P)H Quinone Dehydrogenase 1	30868	1368
CELF1	CUGBP Elav-Like Family Member 1	52063	1312
NRXN1	Neurexin 1	161883	1256
CNTNAP2	Contactin Associated Protein 2	148167	1221
MEF2C	Myocyte Enhancer Factor 2C	51221	1192
NLK	Nemo Like Kinase	58283	1143
MBD5	Methyl-CpG Binding Domain Protein 5	159895	1096
FOXG1	Forkhead Box G1	52352	1067
CHD8	Chromodomain Helicase DNA Binding Protein 8	290519	1003
IRF8	Interferon Regulatory Factor 8	48356	987
CDKL5	Cyclin Dependent Kinase Like 5	115538	967
EHMT1	Euchromatic Histone Lysine Methyltransferase 1	141466	944
SLC9A7	Solute Carrier Family 9 Member A7	80131	890
FERMT2	Fermitin Family Member 2	77861	844
MBNL1	Muscleblind Like Splicing Regulator 1	41817	812
TNIK	TRAF2 And NCK Interacting Kinase	154943	802
LOXHD1	Lipoxygenase Homology Domains 1	235677	779
KIF13A	Kinesin Family Member 13A	202308	746
FN1	Fibronectin 1	272320	732
LAMC1	Laminin Subunit Gamma 1	177603	712
PITX2	Paired Like Homeodomain 2	35370	692
FOXD3	Forkhead Box D3	47630	683
SOX9	SRY-Box Transcription Factor 9	56137	671
KRT20	Keratin 20	48487	663
MAD2L2	Mitotic Arrest Deficient 2 Like 2	24334	632
ZIC3	Zic Family Member 3	50569	612
TJP1	Tight Junction Protein 1	195459	594
NFE2L2	Nuclear Factor, Erythroid 2 Like 2	67827	576
MBNL2	Muscleblind Like Splicing Regulator 2	40518	546
VSX1	Visual System Homeobox 1	38431	512
EVA1A	Eva-1 Homolog A, Regulator Of Programmed Cell Death	17470	498
DRAM1	DNA Damage Regulated Autophagy Modulator 1	26253	477
TXNL1	Thioredoxin Like 1	32251	465
ID2	Inhibitor Of DNA Binding 2	14917	415

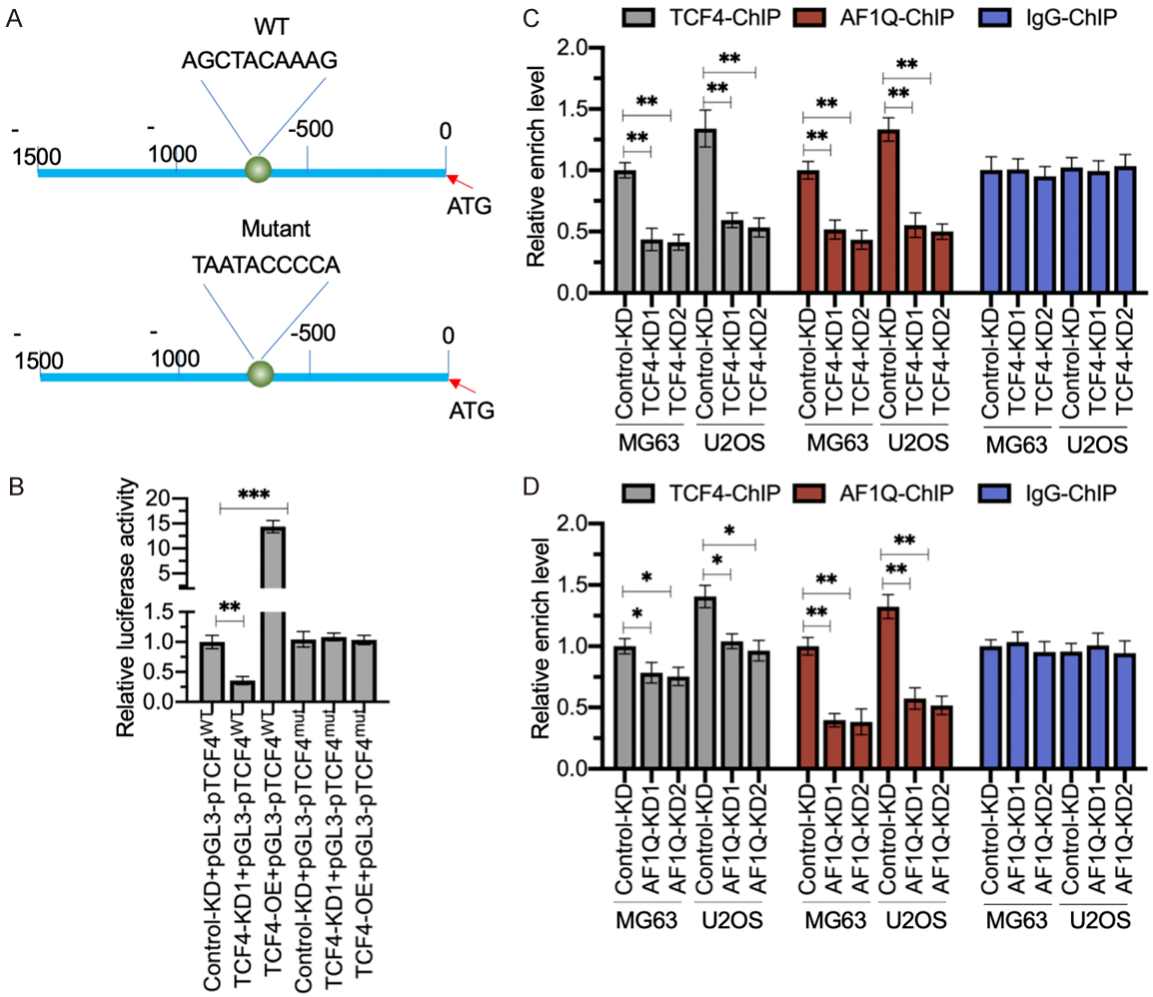

Figure S2. The AF1Q-TCF4 complex was responsible for the regulation of *COX2*. A. The WT and mutated promoters of *COX2*. The schematic diagrams of WT and mutated promoters of *COX2* and the mutated sequence was shown. B. Luciferase assay result. The pGL3-pTCF4^{WT} + Renilla and pGL3-pTCF4^{mut} + Renilla plasmids were transfected into Control-KD, TCF4-KD1 and TCF4-OE cells in the MG63 background, respectively. The transfected cells were used for luciferase assay. $^{**}P < 0.01$ and $^{***}P < 0.001$. C. ChIP results in TCF4-KD cells. The Control-KD and TCF4-KD (#1 and #2) cells in both MG63 and U2OS backgrounds were subjected to ChIP assays using anti-TCF4, anti-AF1Q, and IgG. $^{**}P < 0.01$. D. ChIP results in AF1Q-KD cells. The Control-KD and AF1Q-KD (#1 and #2) cells in both MG63 and U2OS backgrounds were subjected to ChIP assays using anti-TCF4, anti-AF1Q, and IgG. $^{*}P < 0.05$ and $^{**}P < 0.01$.

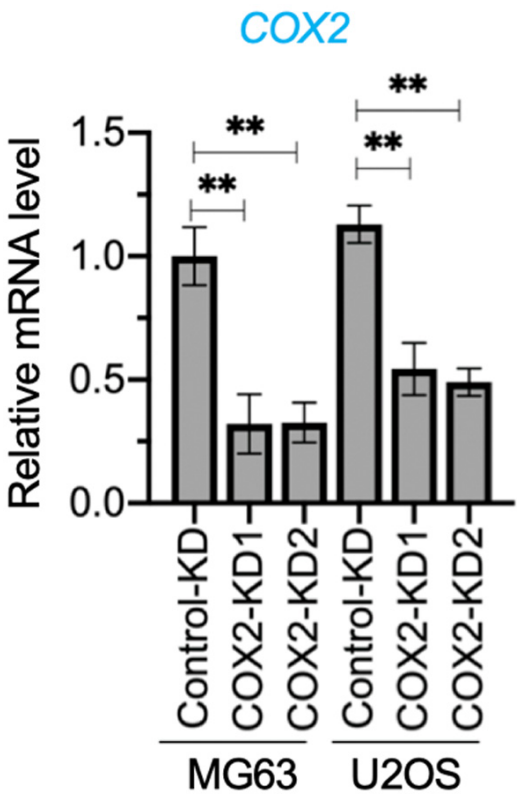

Figure S3. The mRNA level of *COX2* in COX2-KD cells. Total RNA samples from Control-KD and AF1Q-KD (#1 and #2) in both MG63 and U2OS backgrounds were subjected to RT-qPCR to examine the mRNA level of *COX2*. $^{**}P < 0.01$.

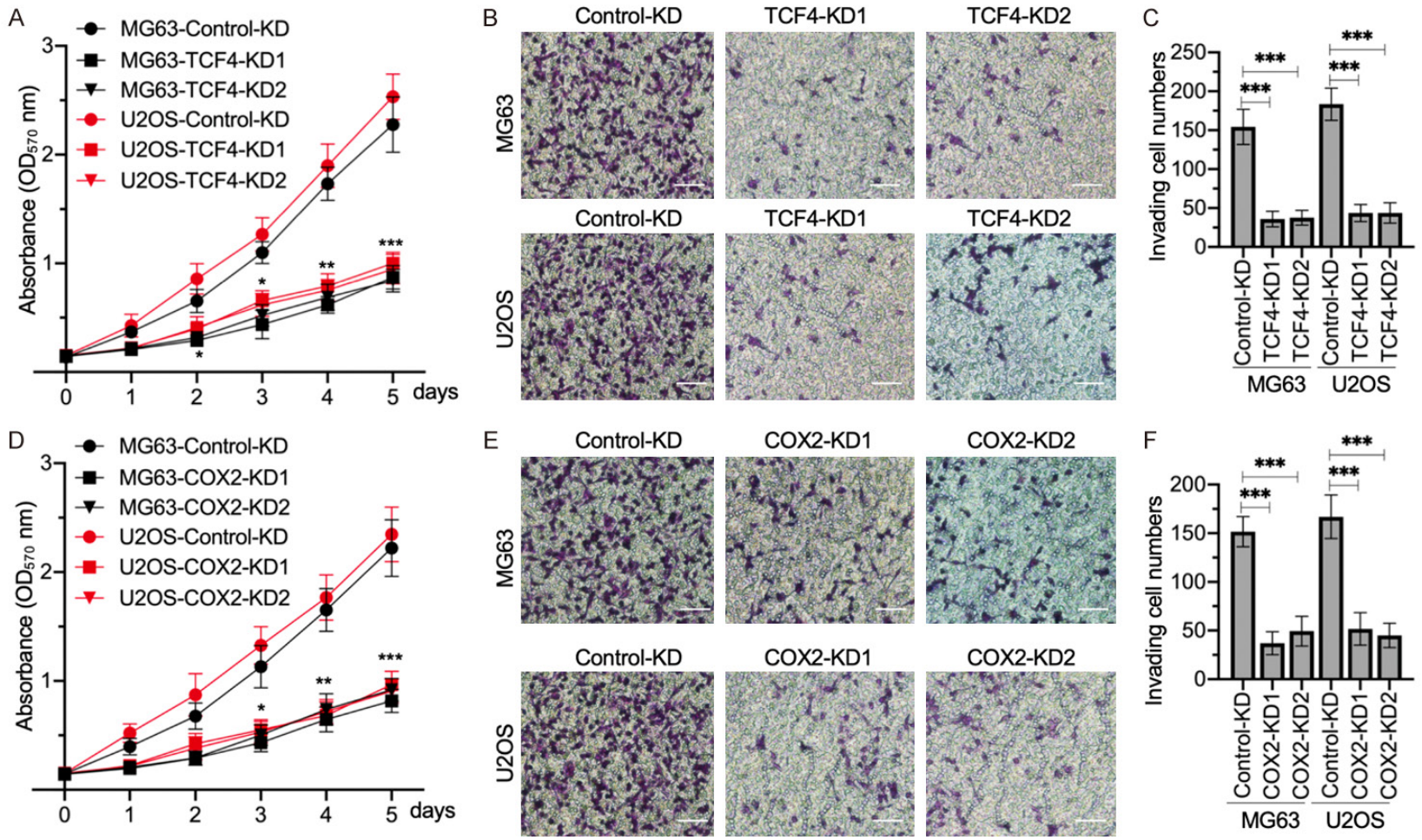

Figure S4. Knockdown of either *TCF4* or *COX2* decreased cell proliferation and invasion. (A) MTT assay in TCF4-KD cells. The Control-KD and TCF4-KD (#1 and #2) cells in both MG63 and U2OS backgrounds were subjected to determine cell proliferation using the MTT method at different time points. **P* < 0.05, ***P* < 0.01, and ***P* < 0.001. (B and C) Cell invasion in TCF4-KD cells. Cells showing in (A) were subjected to the Boyden Chamber assay and the invaded cells were stained using 0.1% crystal violet (B). The crystal violet-positive cells were counted by Image J software (C). (D) MTT assay in COX2-KD cells. The Control-KD and COX2-KD (#1 and #2) cells in both MG63 and U2OS backgrounds were subjected to determine cell proliferation using the MTT method at different time points. **P* < 0.05, ***P* < 0.01, and ***P* < 0.001. (E and F) Cell invasion in COX2-KD cells. Cells showing in (D) were subjected to the Boyden Chamber assay and the invaded cells were stained using 0.1% crystal violet (E). The crystal violet-positive cells were counted by Image J software (F). Bars = 100 μm.

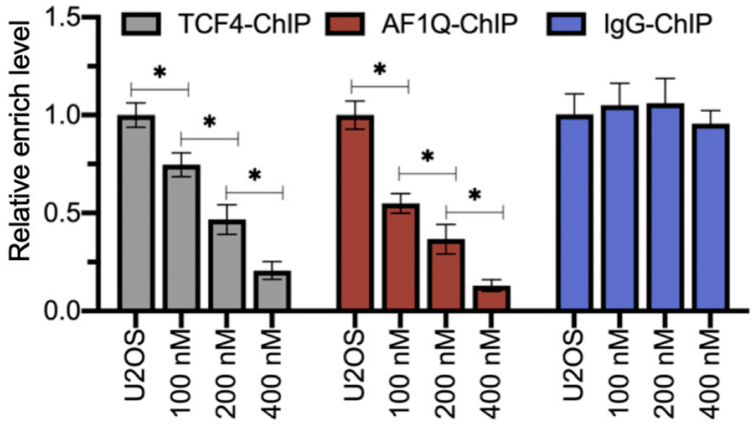

Figure S5. PSM0537 impaired the binding of AF1Q-TCF4 complex on the promoter of *COX2*. The U2OS cells were treated with different concentrations of PSM0537 (0, 100, 200, and 400 nM), followed by ChIP assays using anti-TCF4, anti-AF1Q and IgG, respectively. The input and output DNA were subjected to RT-qPCR. *$P < 0.05$.

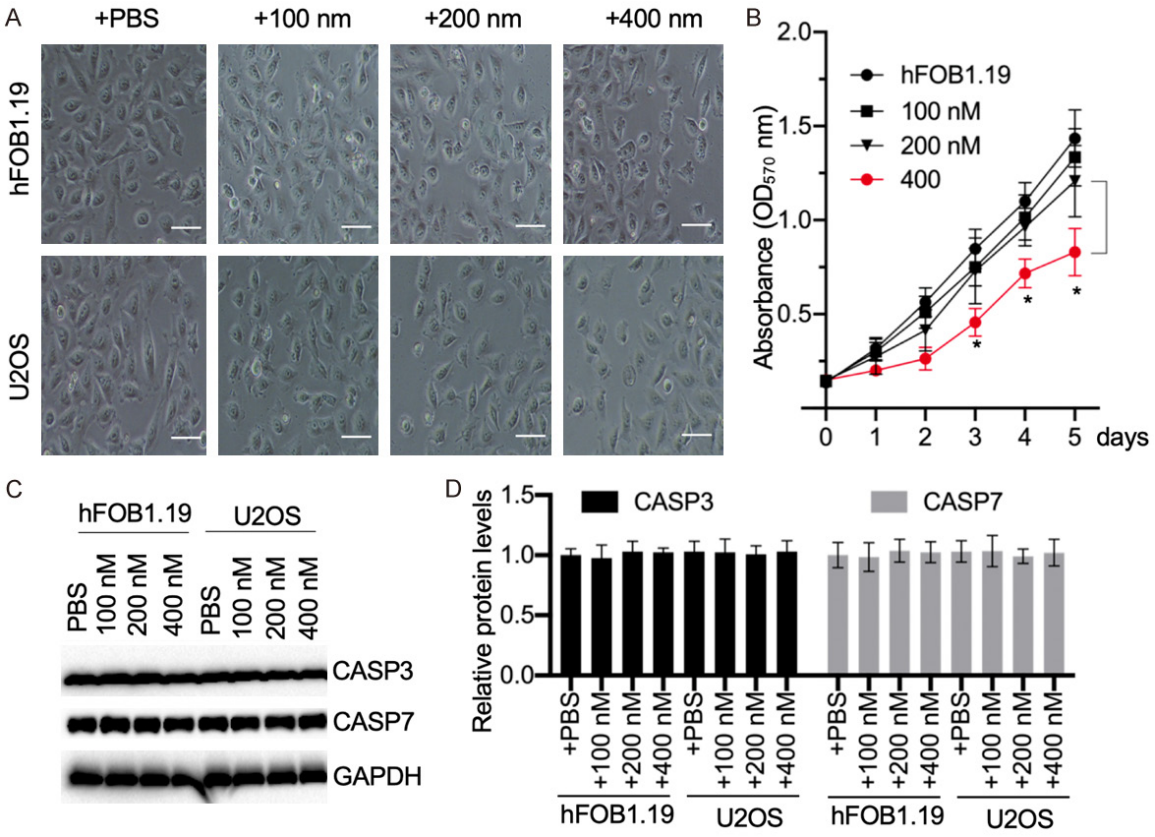

Figure S6. PSM0537 had a low cytotoxicity to hFOB1.19 cells. (A) Cell morphology with PSM0537 treatments. The hFOB1.19 and U2OS cells were treated with different concentrations of PSM0537 (0, 100, 200, and 400 nM) for 24 hours. Cells were photographed. Bars = 200 nm. (B) Cell proliferation results. The hFOB1.19 cells were treated with different concentrations of PSM0537 (0, 100, 200, and 400 nM) and then subjected to determine cell proliferation using the MTT method at different time points. *$P < 0.05$. (C and D) Protein levels of CASP3 and CASP7. Cells as shown in (A) were lysed and subjected to western blotting to examine protein levels of CASP3, CASP7, and GAPDH (loading control) (C). The intensity of the protein bands was quantified and normalized to GAPDH (D).

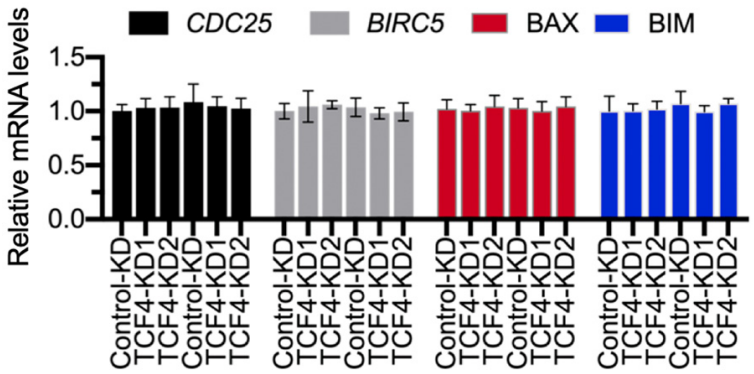

Figure S7. The mRNA levels of *CDC25*, *BIRC5*, *BAX* and *BIM* in TCF4-KD cells. The RNA samples used in **Figure 4D** were subjected to RT-qPCR analyses to examine mRNA levels of *CDC25*, *BIRC5*, *BAX* and *BIM*.